U.S. DEPARTMENT OF THE INTERIOR

U.S. GEOLOGICAL SURVEY

Currents over the Slope off San Francisco, California

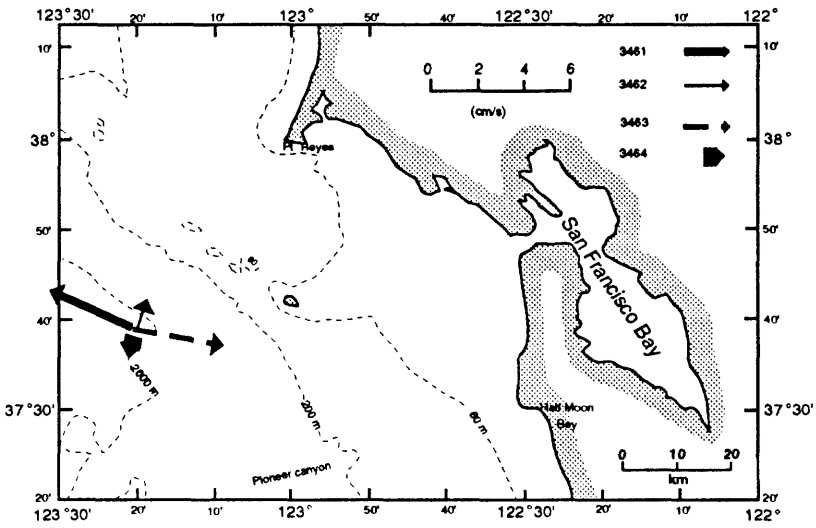

by

Marlene Noble[1] and Kaye Kinoshita[1]

Open-File Report 92-555

Prepared in cooperation with the U.S. Navy

[1]U. S. Geological Survey, Menlo Park, CA, 94025

TABLE OF CONTENTS

LIST OF FIGURES

INTRODUCTION

The region of the coastal ocean over the slope off San Francisco Bay is an important commercial and recreation resource. Major shipping lanes traverse the slope. Commercial and sports fisherman are regularly found in the area. Sites for the testing of submarines and the historic disposal of chemical and munitions materials are found at several deep-water locations. But until recently, very little was known about either the geology or the currents in the region. In particular, no long-term measurements of currents over this region of the slope have been reported in the published literature.

In the past few years, interest in processes over the slope off San Francisco has increased markedly because selected regions of the slope have been proposed as possible sites for the disposal of material dredged from San Francisco Bay. The Navy has requested that an abandoned chemical munitions dumping area on the slope be reactivated as a site for the disposal of some of the dredged materials. As part of their proposal, the Navy has asked scientists from the U. S. Geological Survey to deploy a mooring on the slope to measure currents in the area of interest. This report describes the data gathered during that deployment.

Data Set

The topography of the slope off San Francisco Bay is very complex (Fig. 1). Isobaths with depths between 200 and 400 m are aligned along 325°. The deeper isobaths are also aligned along 325° for length scales longer than 30 km. But on smaller scales, the deeper isobath can change orientation by as much as 90° because seamounts and submarine canyons are found in this area. Pioneer Seamount is the largest seamount. It rises from a depth of 2800 m to 1000 m (Fig. 1). The adjacent Pioneer Canyon cuts across the entire slope to head in depths less than 200 m.

A small submarine canyon cuts into the slope at 37° 40' N. The canyon walls are 400 m high near the mouth of the canyon and shrink to less that 100 m high near the head of the canyon. The orientation of the canyon axis ranges from 45° near the mouth, to 135° in middle, and back to 45° near the head of the canyon. The shallower portions of this canyon are within the boundaries of the Gulf of the Farallones Marine Sanctuary. The deeper portions of the canyon outside the sanctuary have been used as a disposal site by the U. S. Navy (Fig. 1).

In July, 1990, a single current meter mooring was deployed in this small canyon for 45 days. The mooring contained 5 EG&G Vector Averaging Current Meters (VACMs). These instruments monitored the current velocity and temperature in the waters above and within the canyon. The current meters were moored at 285, 485, 885, 1685 and 2495 m below the surface of the water (Table 1). The deepest current meter was 30 m above the sea floor, well within the canyon. All other instruments were located above the rim of the canyon. A complete set of current and temperature data was recovered from the top 4 current meters. The current sensor failed on the lowest current meter; only temperature records were obtained at this site (Table 1).

The currents were decomposed into an alongslope and onslope coordinate system. The positive alongslope direction was toward the northwest at 325° (Table 1). The positive onslope direction was toward the coast, at 55°. This orientation of the currents is aligned with the general trend for isobaths on the slope. A time series of subtidal currents was obtained through use of a low-pass filter with a half-power point at 33 hours (Beardsley, et al., 1985).

Table 1. Description of a current-meter mooring located at 37° 38.1'N , 123° 21.1'W.

Station	Depth		Alongslope Orientation	Variables	Observation Period
	Instrument	Water			
3461	285 m	2525 m	325°	C, T	7 July 1990
					21 August 1990
3462	485 m	2525 m	325°	C, T	7 July 1990
					21 August 1990
3463	885 m	2525 m	325°	C, T	7 July 1990
					21 August 1990
3464	1685 m	2525 m	325°	C, T	7 July 1990
					21 August 1990
3465	2495 m	2525 m	325°	T	7 July 1990
					21 August 1990

Table 2. Basic statistics for each measurement site. The error bars around the mean are given at the 95% confidence level.

	Along-slope (cm/s)	Cross slope (cm/s)	Speed (cm/s)	Temperature (degrees C)
		3461		
Mean	3.1 ± 6.0	-1.9 ± 6.0	-	8.1 ± 0.2
Standard Dev.	7.2	6.9	-	0.3
Minimum	-22.7	-25.2	2.0	7.4
Maximum	24.0	15.7	28.4	8.9
		3462		
Mean	0.5 ± 6.8	0.7 ± 4.9	-	6.3 ± 0.1
Standard Dev	7.3	5.8	-	0.2
Minimum	-21.7	-19.9	1.9	5.8
Maximum	21.6	19.2	23.0	6.8
		3463		
Mean	-3.0 ± 4.6	3.0 ± 2.5	-	4.5 ± 0.1
Standard Dev	6.0	4.3	-	0.1
Minimum	-18.2	-10.8	1.5	4.3
Maximum	16.1	16.6	20.3	4.8
		3464		
Mean	-0.5 ± 2.5	-0.6 ± 1.7	-	2.5 ± 0.0
Standard Dev	3.9	3.4	-	0.0
Minimum	-13.0	-16.2	1.5	2.3
Maximum	15.1	9.6	16.4	2.6
		3465		
Mean	-	-	-	1.8 ± 0.0
Standard Dev	-	-	-	0.0
Minimum	-	-	-	1.7
Maximum	-	-	-	1.9

CTD casts that measure the temperature and salinity of the water column with depth at single points in time were obtained at several locations close to the mooring site when the mooring was deployed and recovered. The measurements show that the main thermocline and pycnocline were located less than 200 m from the sea surface, well above the top instrument on the mooring (Fig. 2). Measurements of the temperature, salinity, and density of the water column over broad areas of the shelf and slope were collected by members of the Naval Postgraduate School while the mooring was in place. The Postgraduate School personnel also collected profiles of currents on the shelf and over the slope. This data is discussed in a separate report (Collins, et al., 1990).

Description of the current field

Average currents

The maximum current speed over the 6 week deployment period was 28.4 cm/s (Table 2); the highest speeds were found at the shallowest measurement site (285 m). The maximum current speed remained above 20 cm/s for depths shallower that 885 m. Maximum currents dropped to 16.4 cm/s at 1685 m. The current speed never dropped below 1.5 cm/s over the deployment period.

The average flow over the 6 weeks of record did not have a constant amplitude or direction (Fig. 3, Table 2). The average flow at 285 m was toward the northwest at 3.6 cm/s; the direction was slightly offshore of the general isobath orientation (325°). The average flow was less than 1 cm/s at 485 m and the direction was toward the north, onshore of the isobath orientation. The average current increased in amplitude and the direction rotated toward the east, again onshore of the slope isobaths, at a depth of 885 m. The average current at the deepest site, 1685 m, was weak and toward the south.

The average currents did not have a statistically stable amplitude or direction at any measurement site (Table 2). Hence, the average directions can not be used to predict the expected direction for the flow in this region of the slope. The directions were not stable because the measurement period was shorter than the time scale for events in the currents. The measurements essentially captured portions of two events. The subtidal currents flowed toward the northwest for the first 3 weeks of record, then toward the southeast for the last 3 weeks (Fig. 4). The subtidal currents tended to flow slightly offshore when the alongslope currents were poleward and onshore when the alongslope flow was equatorward. The average currents over the first and last 3 weeks of record reflect this tendency (Fig. 5). The average current shallower than 500 m flowed poleward and offshore at speeds ranging from 5.9 to 9.7 cm/s for the first half of the record (Table 3).

Table 3. Average current direction and speed for the first (July 9, 1990 - August 1, 1990) and second (August 1,1990 - August 20,1990) half of the record

Station	First half		Second half	
	Direction	Speed (cm/s)	Direction	Speed (cm/s)
3461	287°	9.7	84°	3.8
3462	306°	5.9	108°	6.4
3463	51°	1.8	111°	7.5
3464	277°	2.0	135°	2.5

The average current was equatorward and onshore over the entire mooring, with speeds between 2.5 and 7.5 cm/s, in the latter half of the measurement period.

Subtidal currents (fluctuations with periods longer than 33 hours)

The subtidal fluctuations were strongest in depths shallower than 500 m (Table 4, Fig 4). They accounted for most of the variability in the currents at the 285 and 485 m sites; subtidal fluctuations contained 64 to 77% of the variance in both the along and onslope flow components. The subtidal currents were weaker and accounted for less than 55% of the variability at deeper depths.

Even though the amplitude of the subtidal alongslope flow weakened considerably with depth, the general pattern for the alongslope currents was fairly consistent over the mooring. The alongslope currents had an increasing poleward flow for the first half of the record, then switched to equatorward (Fig. 6a). The correlations between measurements at different depths were above 0.78 for all instrument pairs (Table 5), indicating that over 60% of the subtidal alongslope variance was coupled across the entire mooring. The longest period fluctuation (with a period of about 6 weeks), controlled the correlated portion of the flow field. The subtidal alongslope fluctuations with periods between 3 and 11 days were generally not correlated across the mooring (Fig. 7a). Unfortunately, even though the statistics indicate that the dominant energy in the subtidal alongslope flow was coupled at this particular time, predictions about the coupling for currents at future time periods can not be made. Because subtidal current events had time-scales comparable to the deployment period, the correlations were not significant at the 95% confidence level.

The subtidal onslope currents were not as obviously correlated as the alongslope currents. For measurements taken at the same time, the correlations for instruments separated by more than 600 m in the vertical were less than 0.68. The correlations were weak because events in the subtidal onslope currents tended to occur about 5 days latter at the lowest measurement site (Fig. 6a). When the time of the record at 1685 m was adjusted for this lag, the correlations increased to values between 0.72 and 0.82 (Table 5). Again, it was the longest period fluctuations that dominated the correlated portion of the subtidal onslope flow field. Onslope currents with periods between 3 and 11 days were not correlated (Fig. 7b).

Tidal currents

Tidal currents were obviously present in both components of the current record (Fig. 8), but they were not the dominant fluctuation in the current record. The tides accounted for less than 20% of the variability for measurements at depths less than 500 m (Table 6). The tides were an increasingly important factor at deeper depths, where they accounted for 27 to 38% of the variability. At depths below 850 m, the tidal and subtidal currents shared a nearly equal role in controlling the variability of the currents.

Even though the tides were more influential at deeper depths, they were not necessarily stronger. The amplitudes of the O_1 and K_1 diurnal tides were nearly constant with depth (Table 7). The amplitude of the dominant semi-diurnal tide, M_2, changed with depth. M_2 currents rotated in a clockwise direction and had amplitudes along the major axis of the ellipse of 4.2 and 4.4 cm/s at depths of 285 and 885 m, respectively. The amplitudes were reduced and the rotation sense switched both above and below the 885 m measurement site. M_2 tidal currents rotated counterclockwise and the amplitudes were 2.6 and 2.3 cm/s at 485 and 1685 m, respectively.

The major axes of most of the diurnal and semidiurnal tidal ellipses were oriented 12° to 61° counterclockwise of the average direction for isobaths on the slope (Table 7). Hence, when the tidal currents were maximum and flowing toward the pole, they were moving water and suspended material slightly offshore. A half of a tidal period latter, when they were strong and flowing toward the equator, water was moving slightly onshore. This pattern of water movement is similar to the general pattern found for subtidal currents.

Table 4. Subtidal current variance and the fraction of the variance in the current record that is accounted for by subtidal fluctuations.

Station	Alongslope		Onslope	
	Variance (cm^2/s^2)	Percent of total variance (%)	Variance (cm^2/s^2)	Percent of total variance (%)
3461	32.4	64	34.8	73
3462	41.6	77	21.8	65
3463	19.5	55	5.5	32
3464	5.5	38	2.8	25

Table 5. Correlations among the subtidal currents. Only the onslope current at station 3464 showed a substantial increase in correlation amplitudes when the current records were lagged in time. A positive lag indicated that the currents at the upper site lead those at the lower.

Station pair	Alongslope current	Onslope current	
	Correlation at zero lag	Correlation at zero lag	Correlation at a 5 day lag
3461-3462	0.87	0.89	-
3461-3463	0.78	0.67	-
3461-3464	0.80	0.43	0.82
3462-3463	0.89	0.71	-
3462-3464	0.85	0.39	0.81
3463-3464	0.89	0.13	0.72

Table 6 Fraction of variance in the current record that is accounted for by the tides. The resolution of the tidal band is 1/360 $hours^{-1}$.

	3461		3462		3463		3464	
Tidal Component	Along-slope (%)	Cross slope (%)	Along-slope (%)	Cross slope (%)	Along-slope (%)	Cross slope (%)	Along-slope (%)	Cross slope (%)
O_1	2.7	0.7	1.4	0.6	1.1	1.3	2.4	2.8
K_1	4.0	1.2	4.0	1.4	3.8	2.4	3.2	9.5
M_2	12.1	6.3	5.3	10.9	20.9	29.1	18.5	8.1
S_2	0.8	0.7	1.4	2.7	4.3	5.5	4.9	7.3
Total	19.6	8.9	12.2	15.6	30.2	38.4	28.9	27.6

Table 7. Tidal ellipse parameters. Positive ellipse orientations indicate that the major axis of the ellipse is rotated clockwise from the positive alongshelf direction (325°). A rotation sense denoted by C (A) indicates that the tidal currents rotate in a clockwise (counterclockwise) direction.

Station	Ellipse Orientation	Semi-major Axis (cm/s)	Semi-minor Axis (cm/s)	Rotation Sense
		O_1		
3461	-21°	1.4	0.0	-
3462	-12°	1.1	0.0	-
3463	-45°	0.8	0.2	C
3464	-46°	0.9	0.4	C
		K_1		
3461	-24°	1.9	0.1	A
3462	-21°	1.6	0.1	C
3463	-24°	1.5	0.4	C
3464	-61°	1.2	0.5	C
		M_2		
3461	-28°	4.2	0.1	C
3462	49°	2.6	1.6	A
3463	-37°	4.4	2.0	C
3464	12°	2.3	1.1	A
		S_2		
3461	-23°	0.8	0.1	C
3462	56°	1.3	0.1	C
3463	-37°	1.4	0.7	C
3464	-29°	1.1	0.4	A

DISCUSSION

The data obtained from this initial deployment of a mooring on the slope indicate that the processes that control both the subtidal and tidal currents over the slope have time scales that are longer than the 6 weeks of record. Even though much longer records are needed before one can determine the exact parameters that control the flow over the slope, some general statements about these processes can be inferred from the measured currents.

A strong pulse of poleward flow was observed mainly at depths shallower than 500 m for the first several weeks of the deployment. Episodes of poleward flow were observed less often and for shorter time periods at deeper depths. It is likely that the poleward flow was caused by an offshore movement of the California Undercurrent to a position over the mooring site. Unfortunately, we can not determine if the California Undercurrent is commonly found over the mooring site because previous measurements of the undercurrent in this region of the central California slope do not exist.

The undercurrent has been observed at locations several hundred kilometers to the northwest and southeast of the mooring, at sites off the Russian River and off Monterey, CA. (Winant, et al., 1988; Collins, C. personal communications). Even though many characteristics of the undercurrent have not been measured, we do know that it tends to be located offshore of the 200 m isobath, have the strongest currents above 600 m, and flow toward the pole over most months of the year. The speeds in the undercurrent can reach amplitude of 50 cm/s. The sparse set of data on the undercurrent indicates that it is located close to the shelf break at some times of the year, but that it can be found further offshore. The undercurrent has be seen off Monterey in water depths deeper than 2000 m (Collins, C. personal communications). These depths are similar to the depth of our mooring. Both the direction of flow and the intensification of the subtidal flow toward the surface suggest that the undercurrent was present over the mooring site.

The California current system is located offshore of the California Undercurrent. Again, a sparse historical data set indicates that the California currents are surface intensified and flow toward the equator (Hickey, 1979). It is likely that the California Current System moved over the mooring in the latter portion of the record, for the measured currents flowed toward the southeast. It is probable that the undercurrent moved into shallower depths, closer to the shelf, at this time.

The diurnal tides had a stable amplitude and phase at all measurement sites on the mooring, indicating that the diurnal tides were driven by the surface tide. The surface tide has a constant forcing over the year and we can expect the parameters measured for the diurnal tides to be typical of this region.

The dominant tidal component, the M_2 semidiurnal tide, did not have a constant amplitude with depth at the mooring site. The tidal amplitudes

were 4.2 cm/s at 285 m. They dropped to 2.6 cm/s at 485 m, returned to 4.4 cm/s at 885 m and dropped back to 2.3 cm/s at 1685 m. The rotation sense changed from clockwise to counterclockwise between each instrument. These characteristics suggest that the M_2 semidiurnal tides were controlled by semidiurnal internal waves at tidal frequency, rather than by the surface tide. Semidiurnal internal waves over the slope often have currents that are as large or larger than the surface tide and have time scales than change over periods of several months (Noble, et al., 1987). Hence the characteristics measured for the M_2 tidal constituent may change over the year, but the range of change is limited. It is unlikely that the amplitudes will vary by more than a factor of 4 from those measured during this deployment.

CONCLUSIONS

The data discussed in this report provide an interesting, but somewhat limited, picture of the currents over the slope off San Francisco Bay. The subtidal and tidal current patterns suggest that materials that settle slowly through the water column at this site would be dispersed into an elongated elliptical footprint. The major axis of the footprint would be orientated 10 to 30° counterclockwise from the along isobath orientation. Materials suspended in the water column would move either toward the northwest and offshore, away from the Gulf of the Farallones Marine Sanctuary, or toward the southeast and onshore. It is probable that sand-size and larger materials would not be resuspended at this site. The currents below 800 m were too weak.

However, the data set is too short to enable us to decide if the current patterns found during the deployment are typical of this region. The characteristics of the average and subtidal flow fields were determined by only 2 events. The measured poleward flow had an offshore component. It is a distinct possibility that it could have an onshore component at other times of the year. The tidal currents contributed to the dispersion of material settling through the water column. A major portion of the tidal currents were internal waves at tidal frequency. It is well-know that these waves change both their amplitude and phases over periods of a few months. Hence, subsequent measurements may show that material is dispersed much more or much less that these measurements suggest.

Finally, this data set is was collected at only one site on the slope. At the present time, it is not known how typical this site is of the general area. We will have some assessment of the spatial scale for currents on the slope in the near future, because a supporting program measured the currents over a broad area of the shelf and slope, but at one moment in time, while the mooring was in place (Collins et al., 1990). The integration of the data from these two measurement programs will provide initial information on the spatial scales for slope currents. Additional moored measurements of currents for longer periods of time at at several locations are needed before detailed models of the dispersion of suspended materials in this area can be developed.

ACKNOWLEDGEMENTS

Funds for the data discussed in this report were supplied by the Naval Ocean Systems Center, San Diego Ca from a program headed by R. K. Johnston. We thank the crew of the ship DeSteiguer for helping to set and recover the current-meter mooring. William Strahle, from the U.S. Geological Survey, headed the technical team that designed and prepared the mooring.

REFERENCES

Beardsley, R. C., R. Limburner, L. Rosenfeld, 1985: Introduction, CODE-2 moored array and large scale data report, Technical Report WHOI 85-35, 234 pp., Woods Hole Oceanographic Inst. Woods Hole Ma.

Collins, C., and others, 1990: A preliminary report to the Navy on work done for the dredge disposal EIS, in prep.

Hickey, B. M., 1979: The California current system - hypothesis and facts. Progress in Oceanography, V 8, 191-279.

Noble, M., L. K. Rosenfeld, R. L. Smith, J. V. Gardner, and R. C. Beardsley, 1987: Tidal currents seaward of the northern California continental shelf. Journal of Geophysical Research, V. 92, 1733-1744.

Winant, C. D., R. C. Beardsley and R. E. Davis, 1987: Moored wind, temperature and current observations made during the Coastal Ocean Dynamics Experiments 1 and 2 over the northern California continental shelf and upper slope, Journal of Geophysical Research, V. 92, 1569-1604.

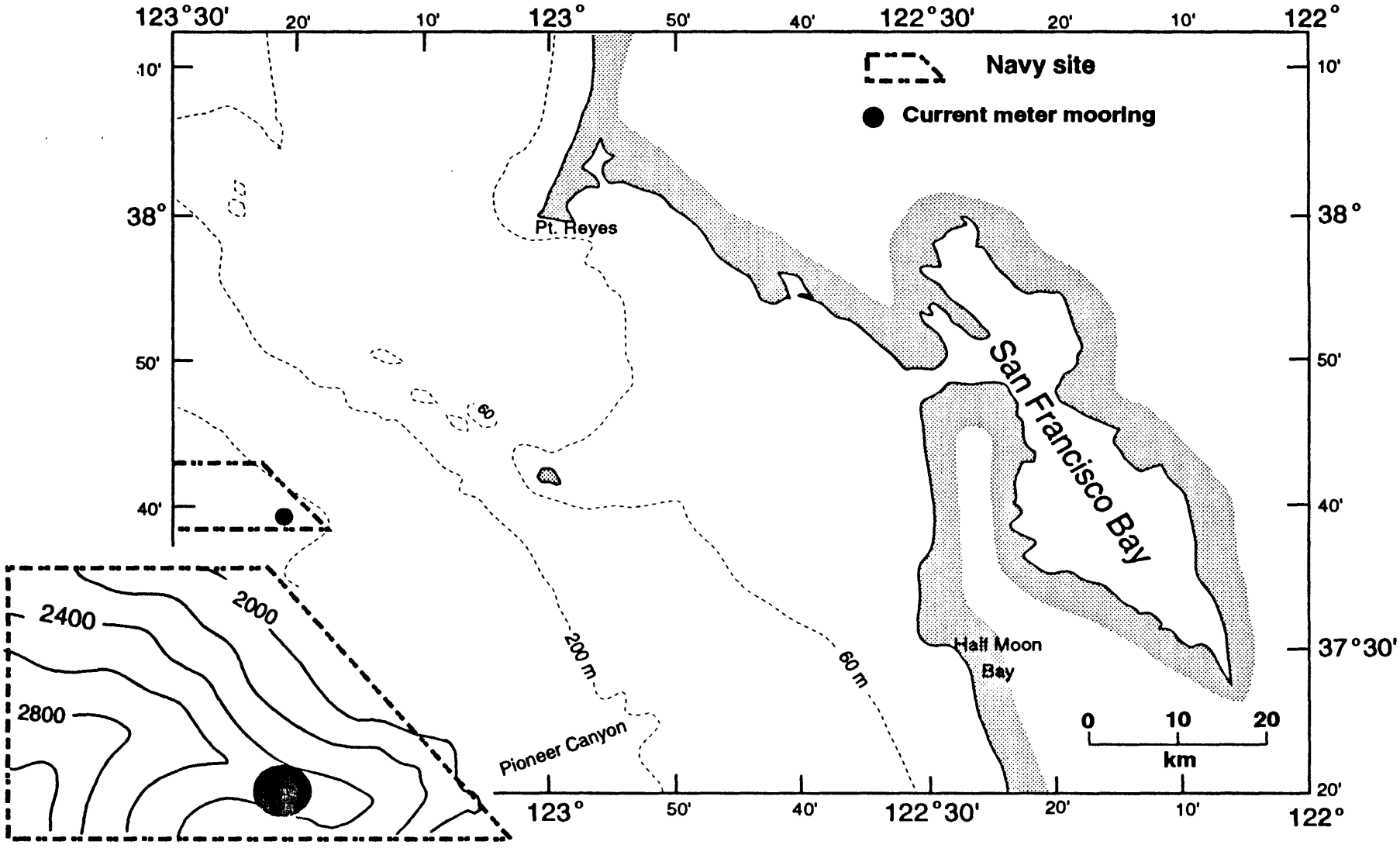

Figure 1. Map of the Gulf of the Farallones. The insert shows details of the topography around the mooring site.

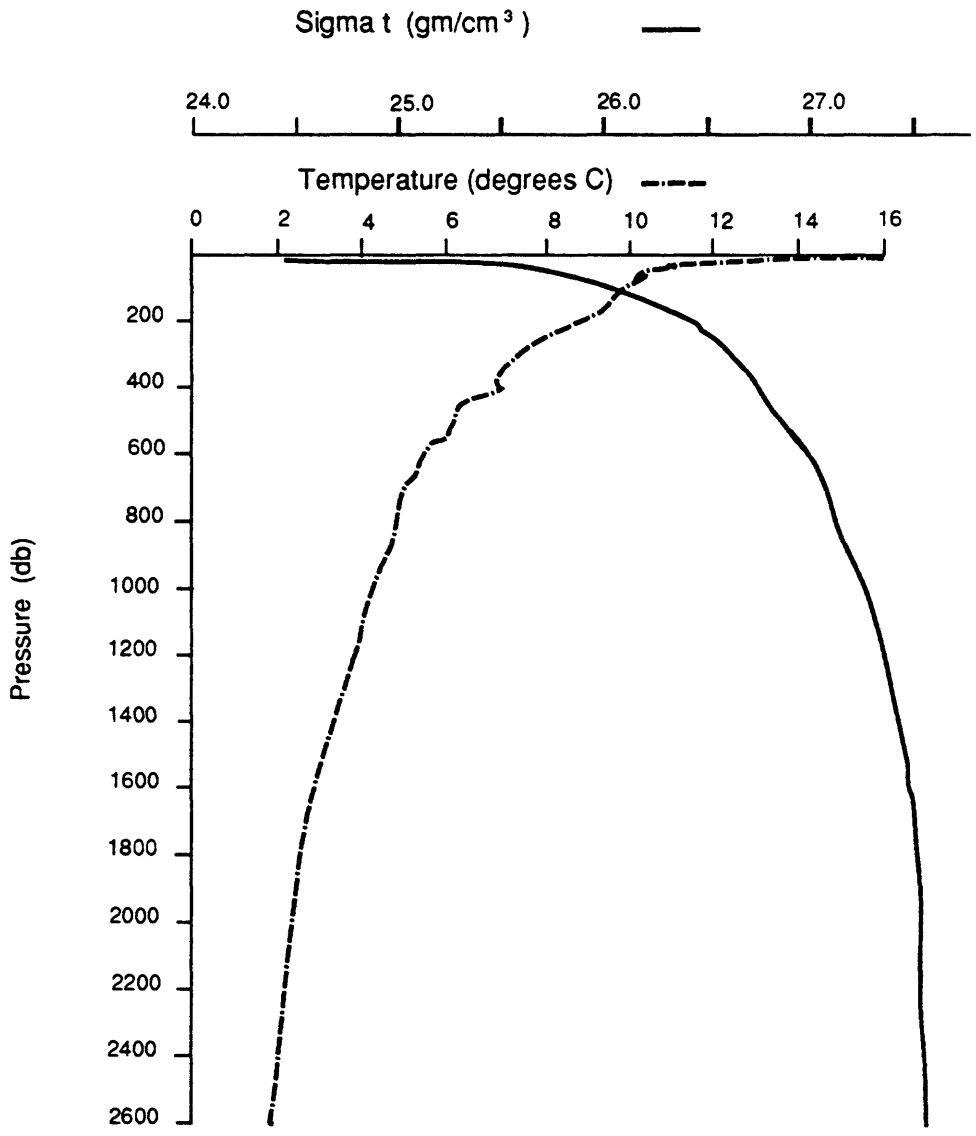

Figure 2. Plot of temperature and density with depth at the mooring site. The measurements were taken when the mooring was recovered.

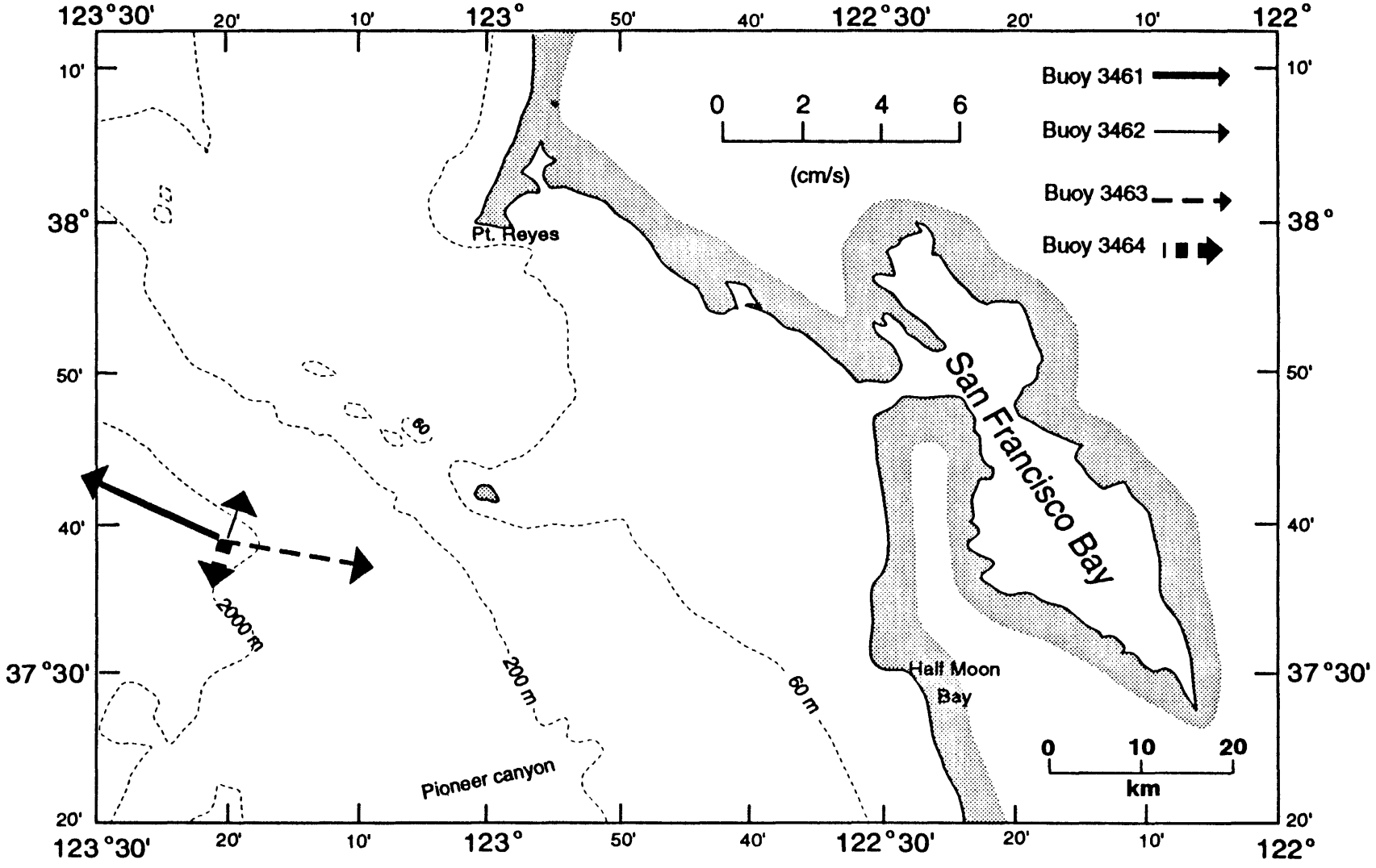

Figure 3. Average currents for the entire record. The depicted directions are not significant at the 95% confidence level.

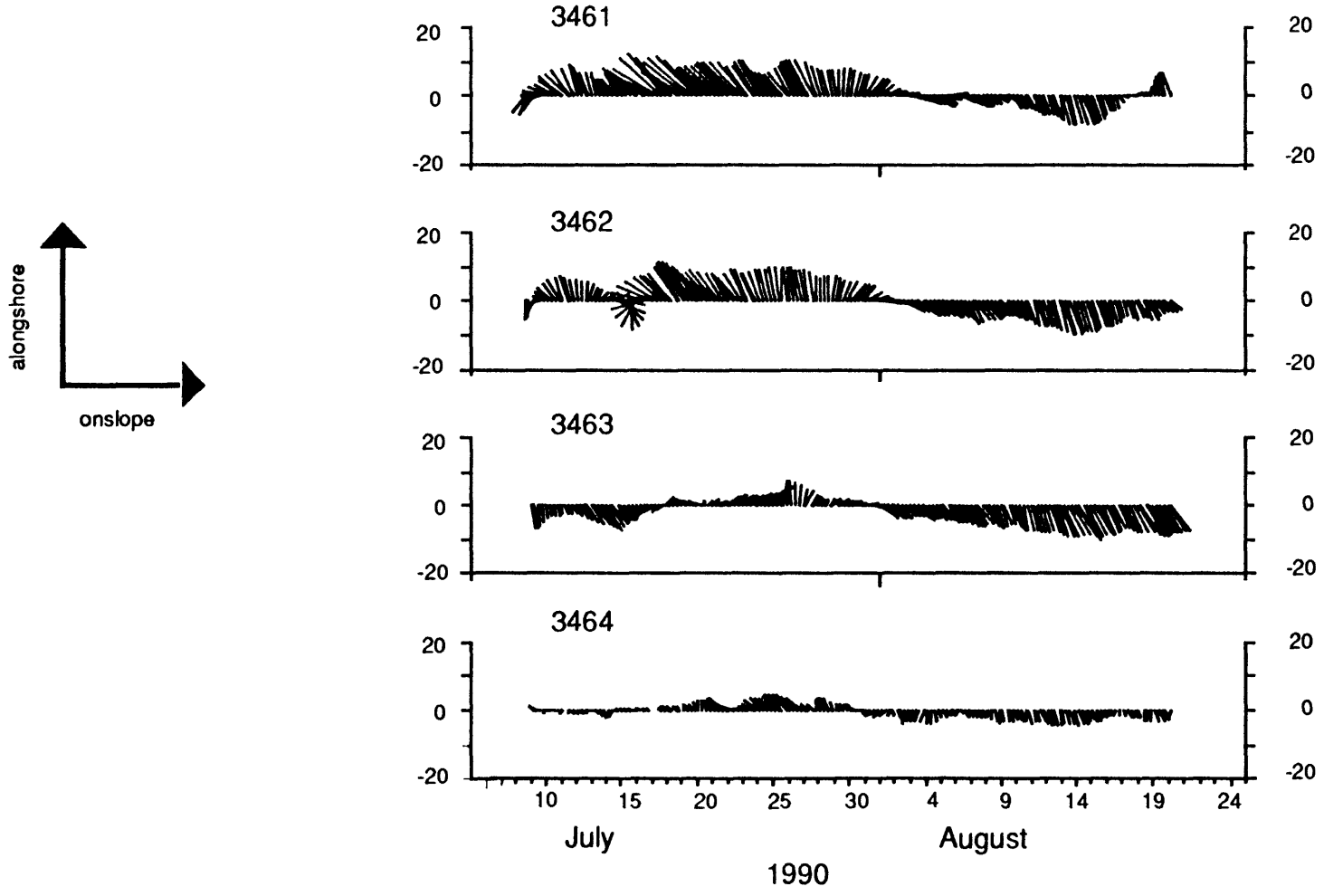

Figure 4. A vector plot of the subtidal currents. Positive alongslope currents are toward 325°. Positive onslope currents are toward 55°.

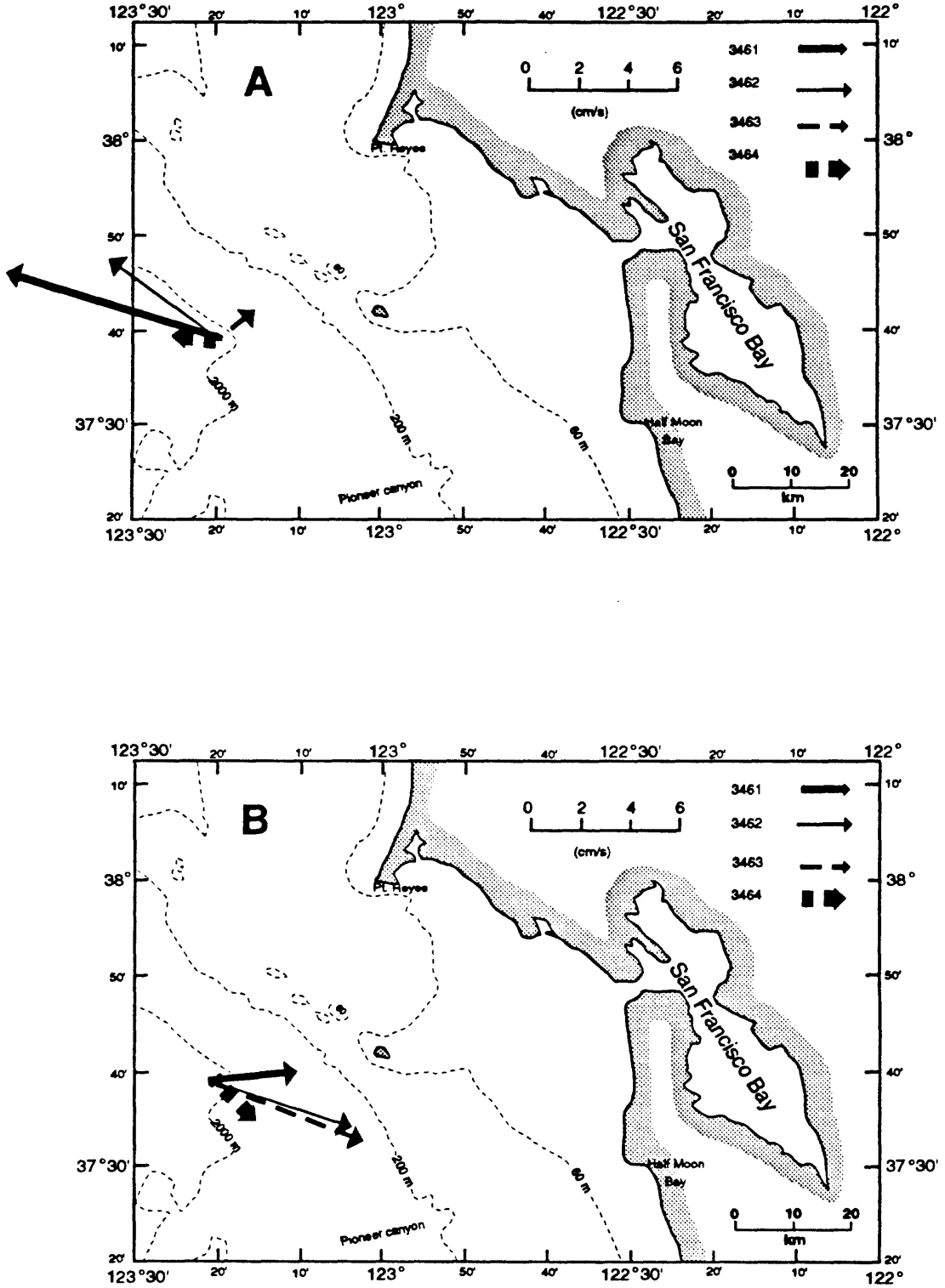

Figure 5. Average currents over the first (A, 900709-900801) and second (B, 900801-900820) half of the current records. The depicted directions are not significant at the 95% confidence level.

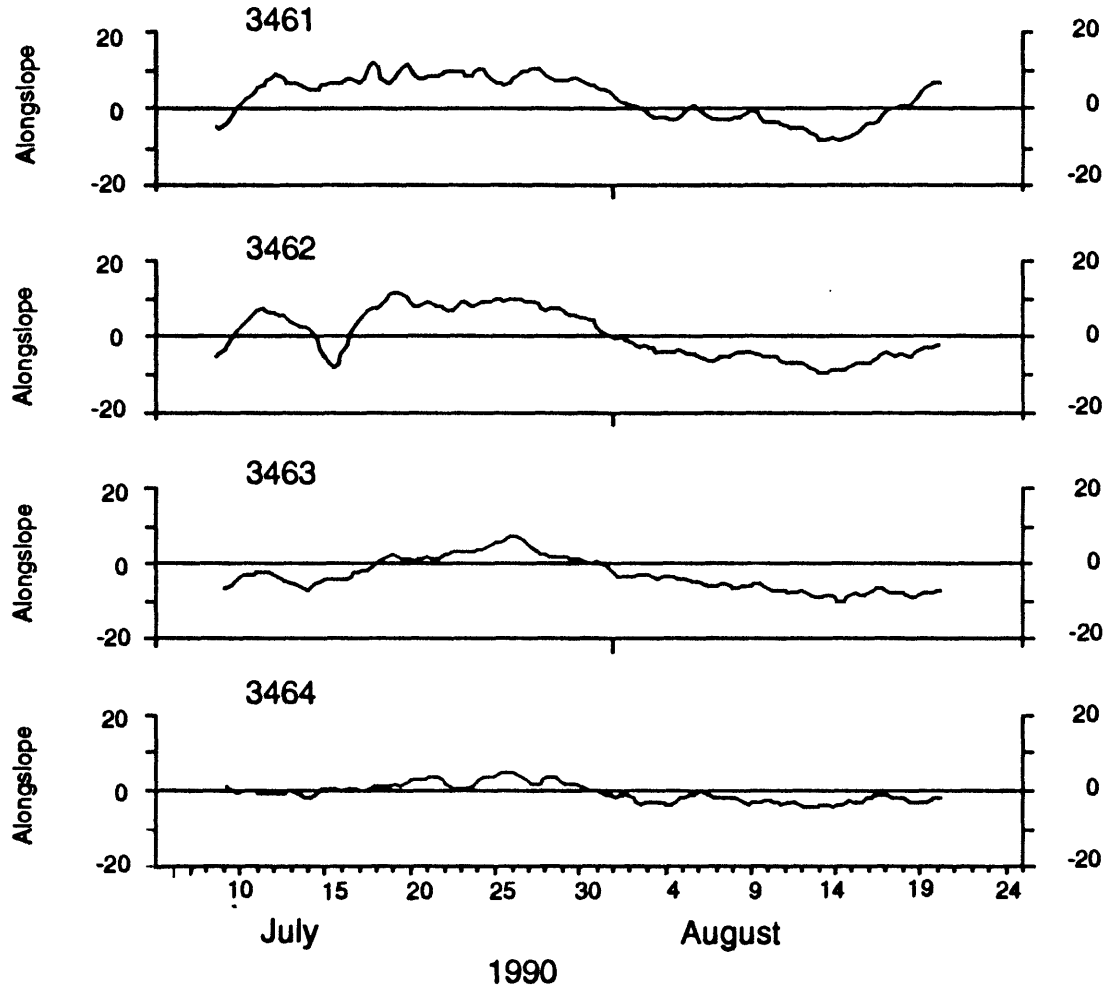

Figure 6a. Subtidal alongslope currents. Positive alongslope currents flow toward 325 °.

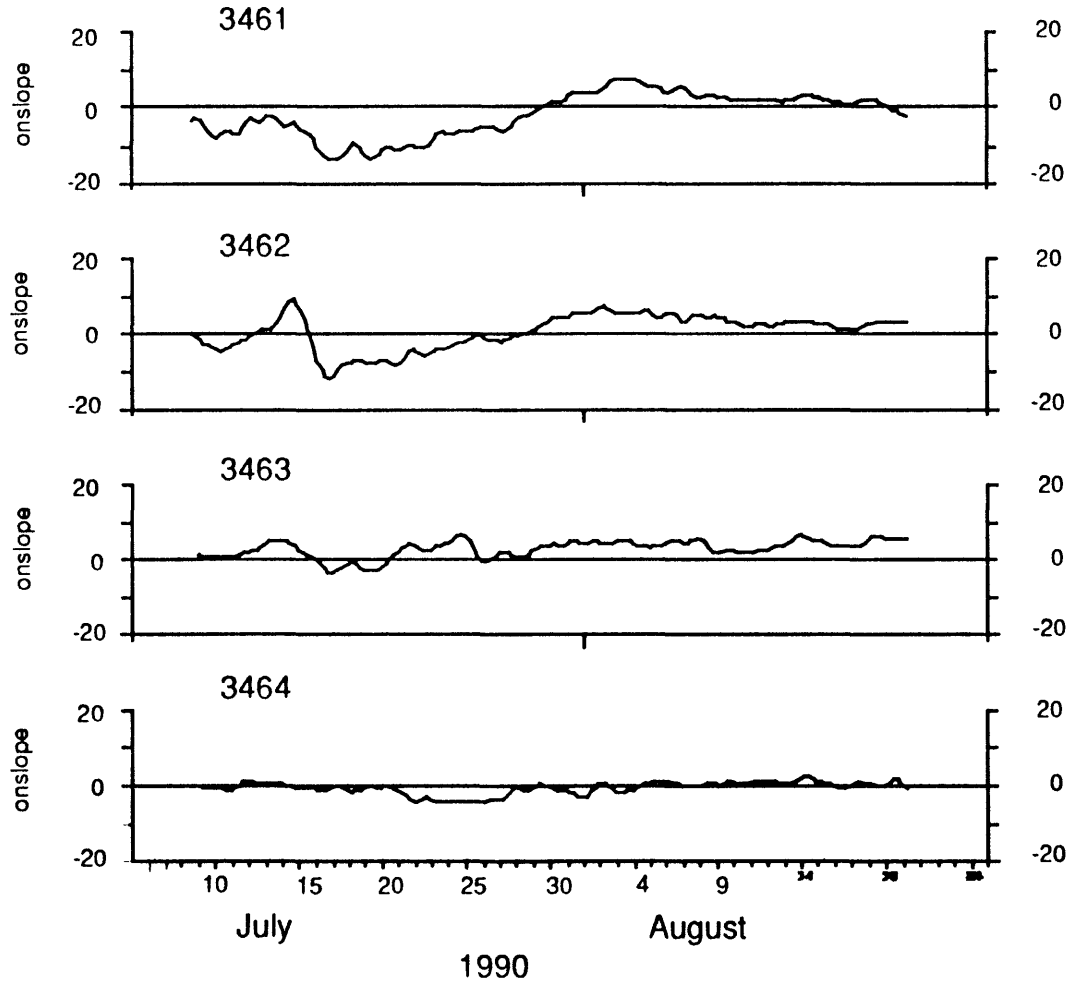

Figure 6b. Subtidal onslope currents. Positive onslope currents flow toward 55°.

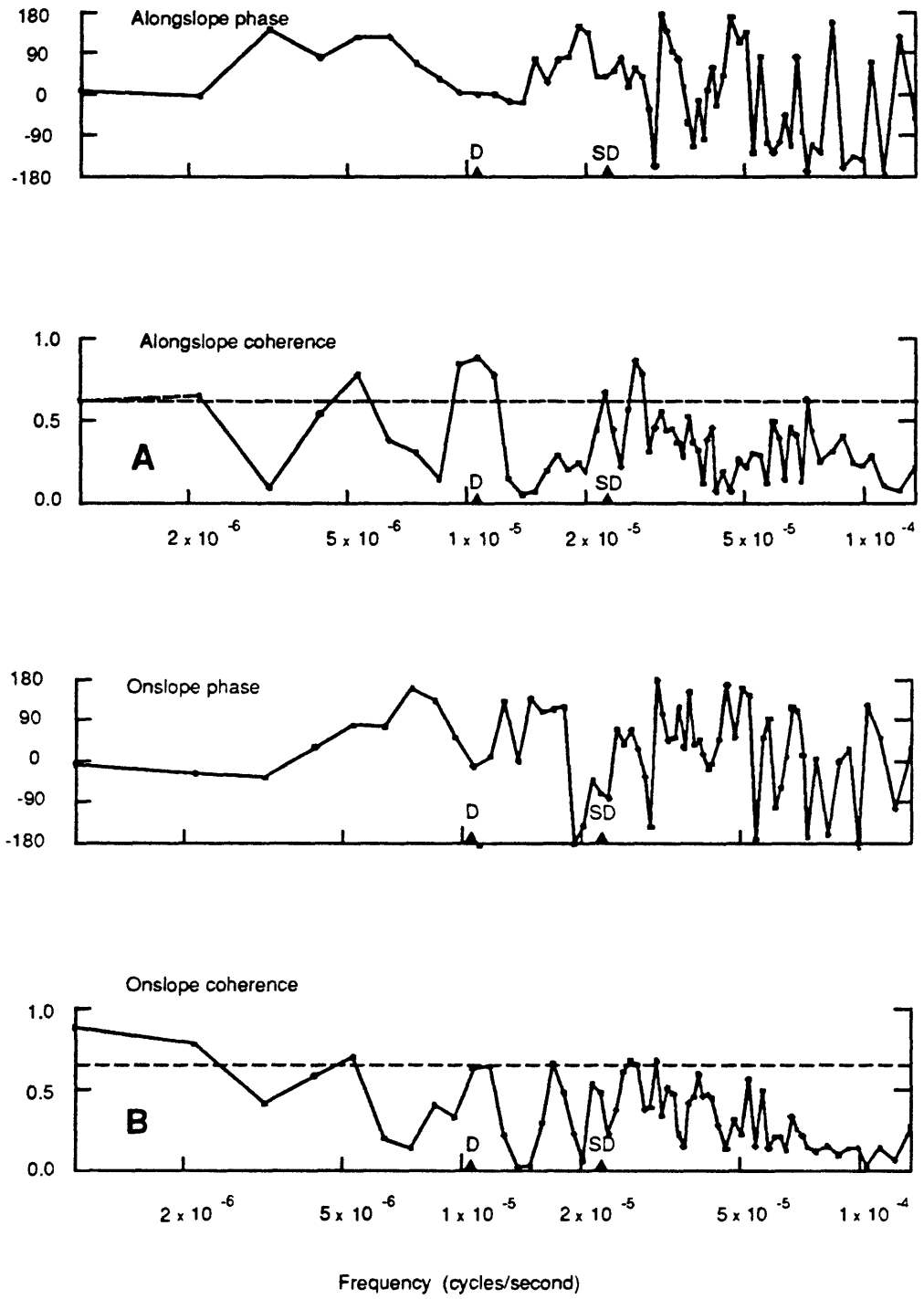

Figure 7. The coherence and phase for alongslope (A) and onslope (B) currents between 285 and 485 m. A positive phase indicates that the currents at 485 m lead currents at 285 m. Coherence levels must be above the dashed line to be significant at the 95% level.

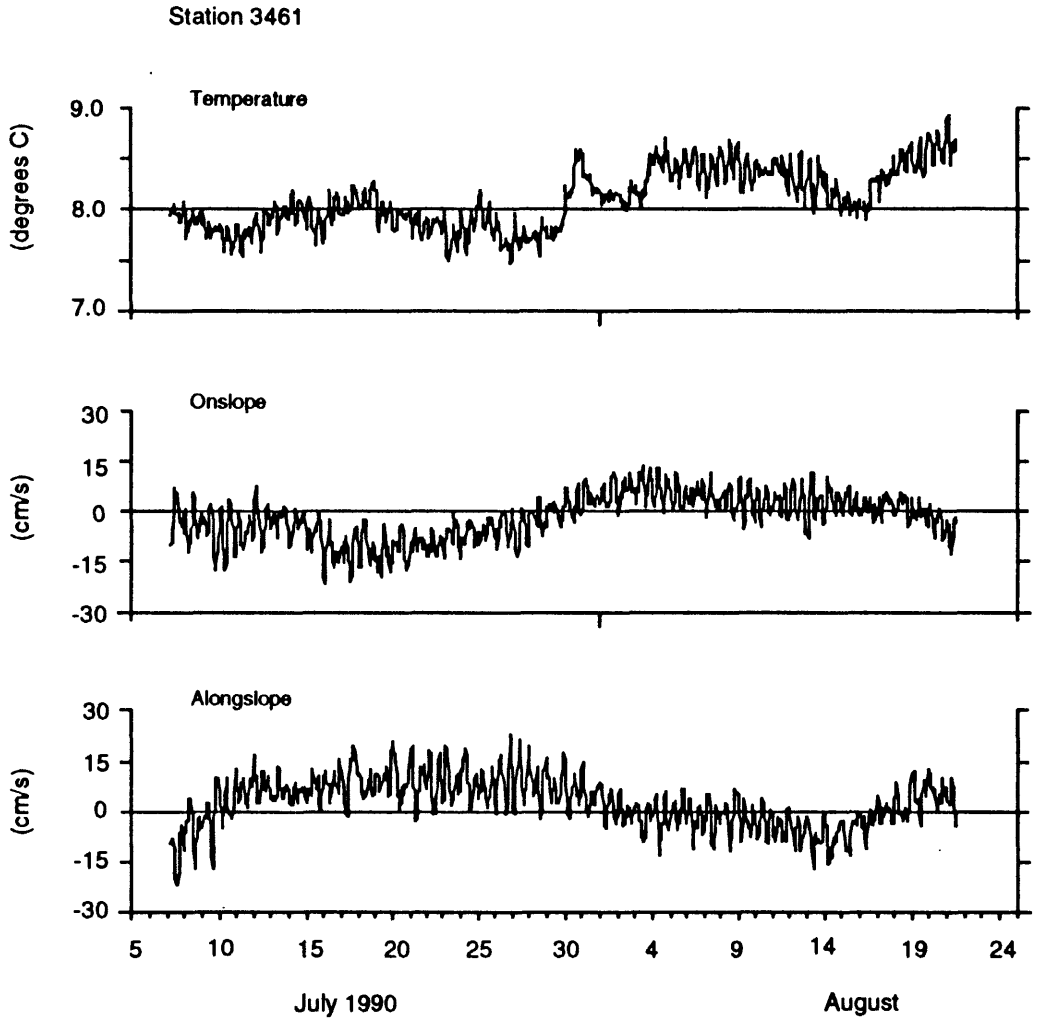

Figure 8. Hour-averaged currents and temperature at 285 m. Positive alongslope currents are toward 325°. Positive onslope currents are toward 55°.

APPENDIX

Time series plots of the subtidal currents and temperatures	Figures A1-A4
Time-series plots of the hour-averaged currents and temperatures	Figures B1-B5
Spectral plots of the hour-averaged currents and temperatures	Figures C1-C13

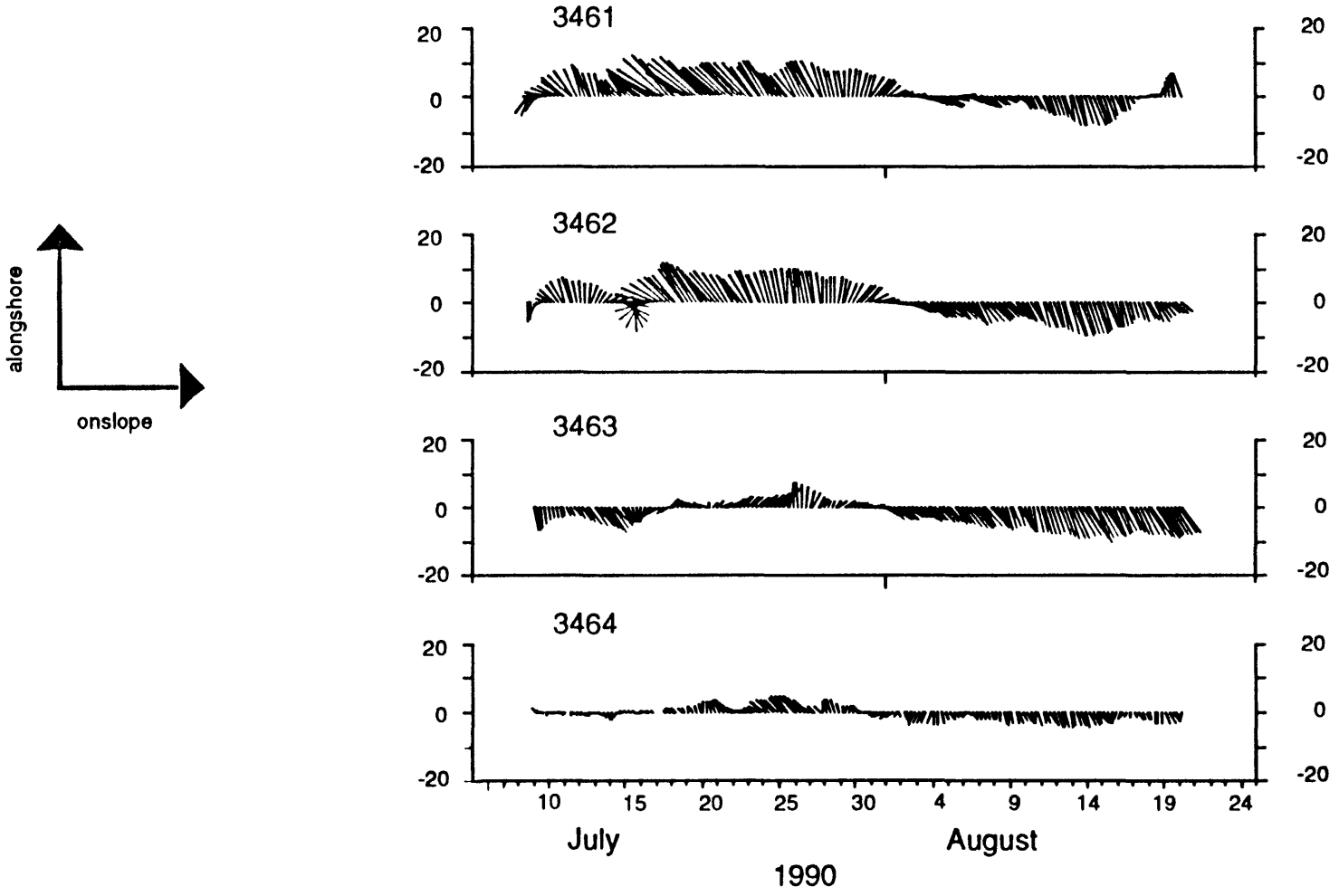

Figure A1. A vector plot of the subtidal currents. Positive alongslope currents are toward 325°. Positive onslope currents are toward 55°.

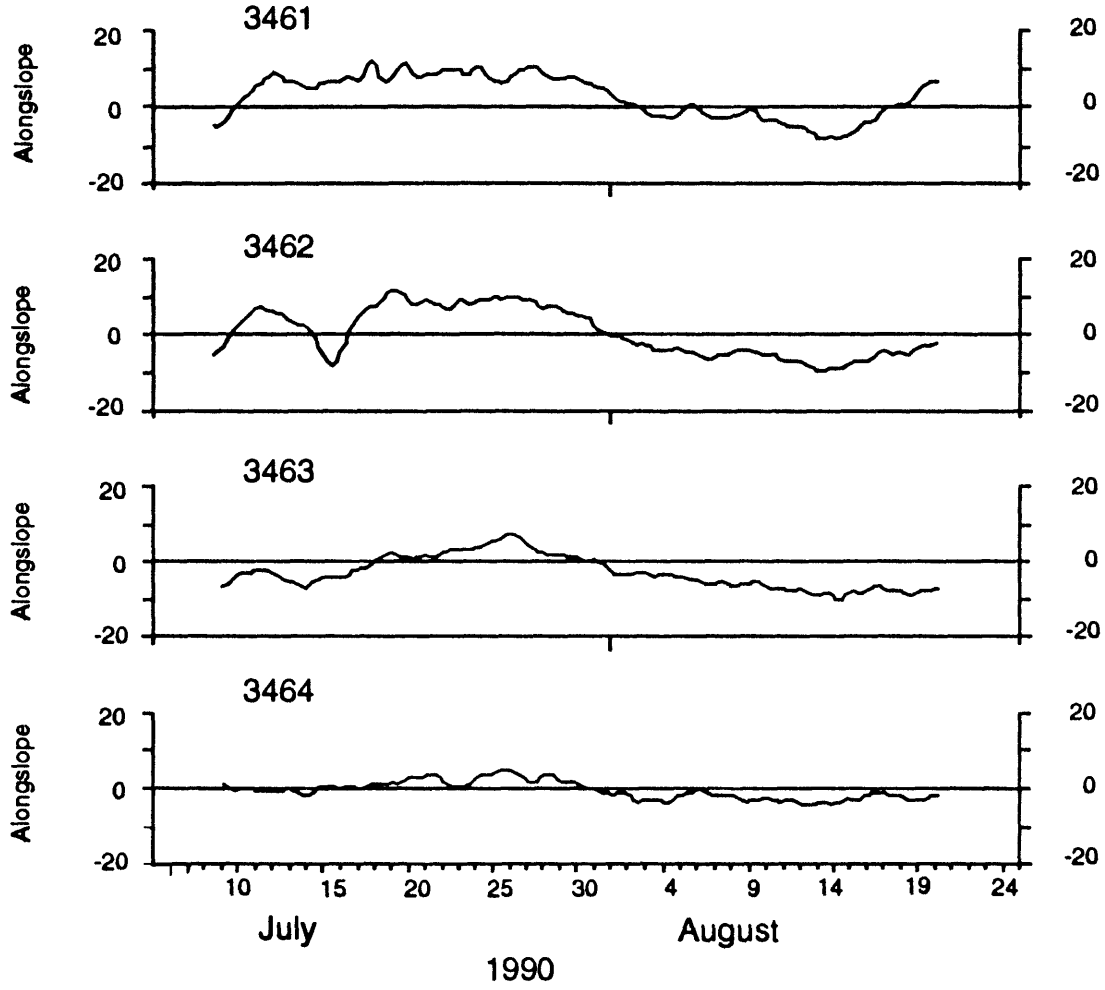

Figure A2. Subtidal alongslope currents. Positive alongslope currents flow toward 325°.

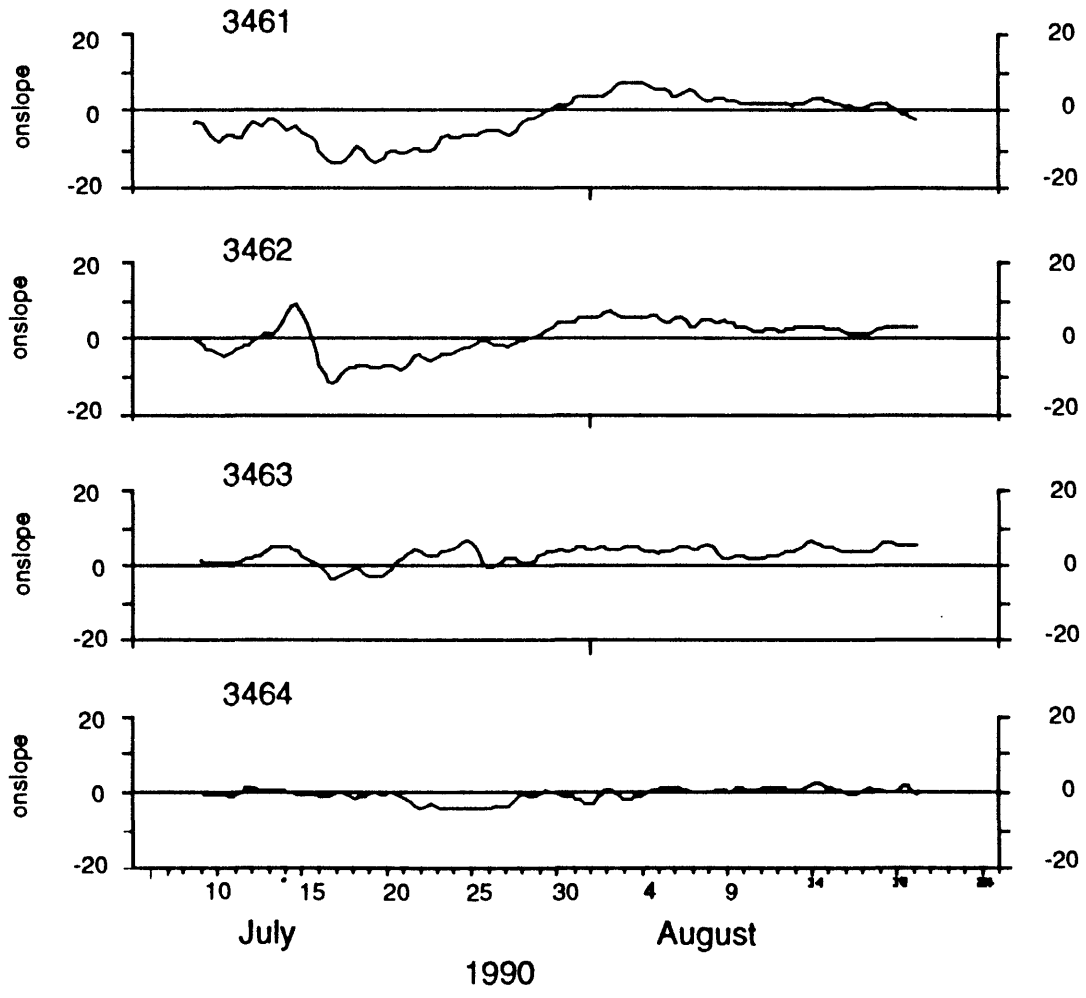

Figure A3. Subtidal onslope currents. Positive onslope currents flow toward 55°.

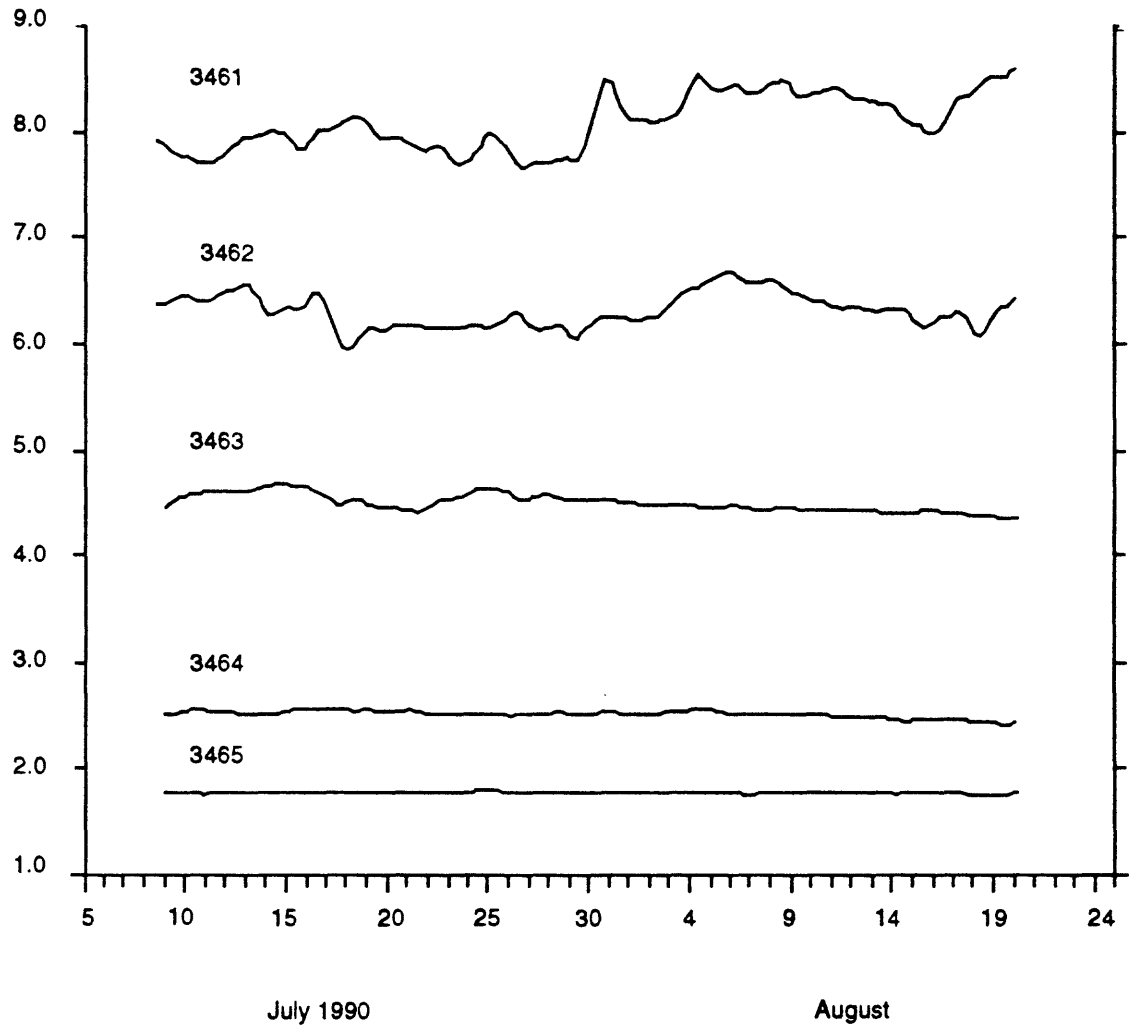

Figure A4. Subtidal temperatures at all measurement sites

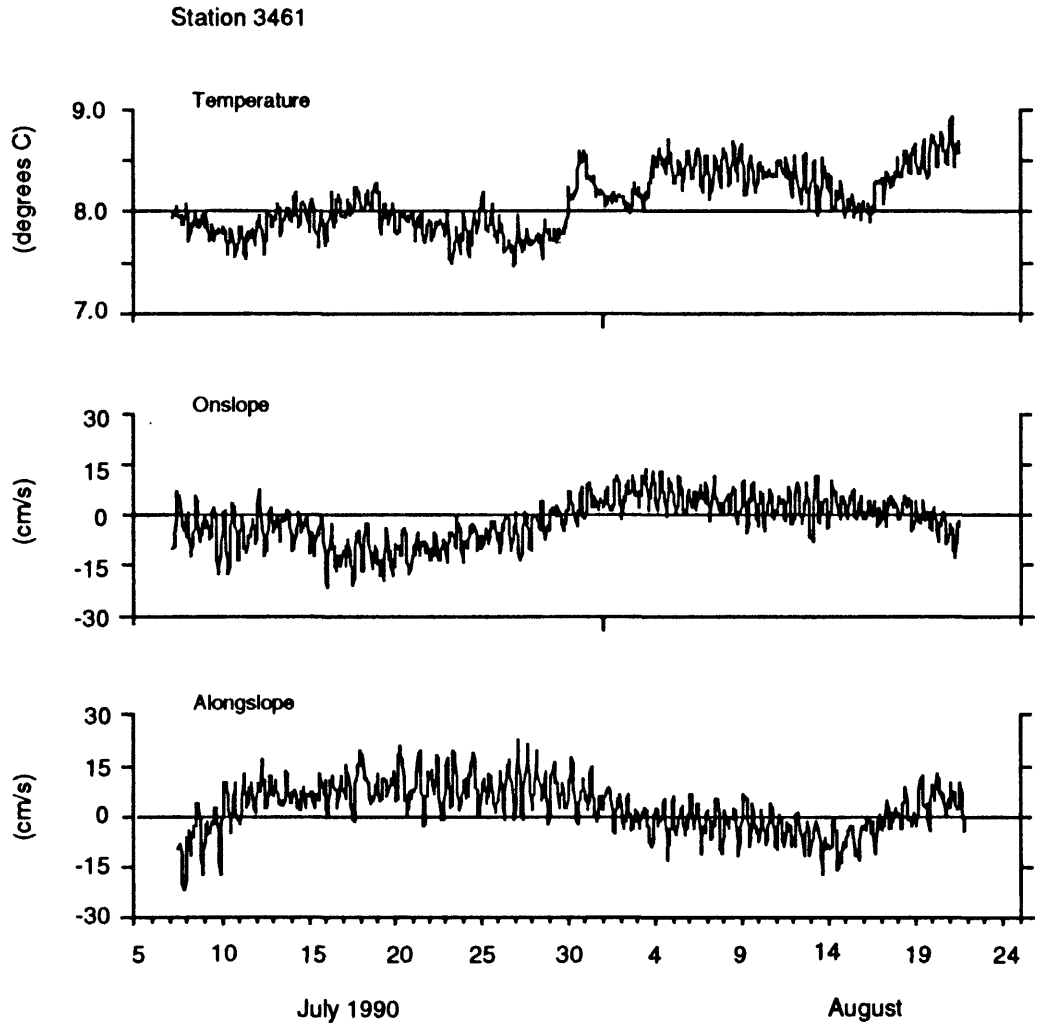

Figure B1. Hour-averaged current and temperature at the 285 m site. Positive along and onslope currents flow toward 325 ° and 55 °.

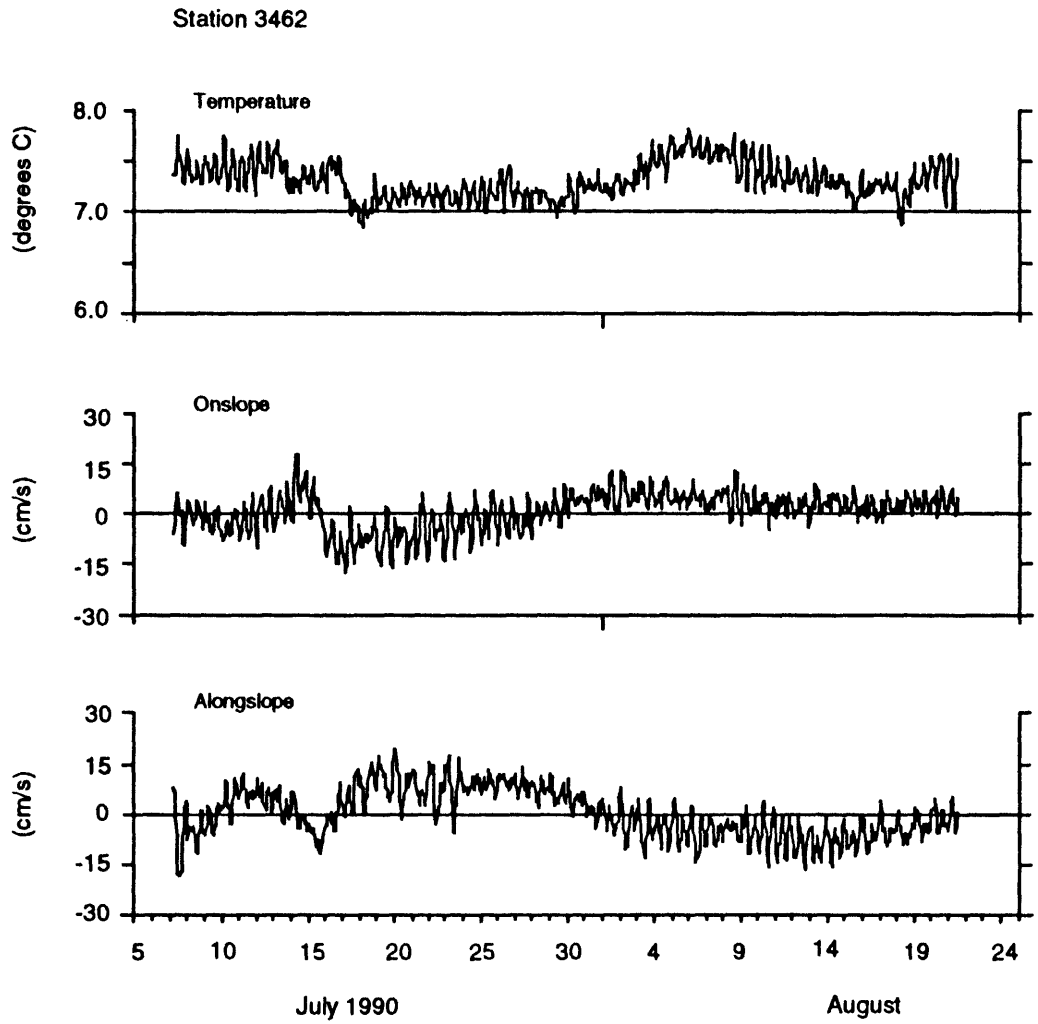

Figure B2. Hour-averaged current and temperature at the 485 m site. Positive along and onslope currents flow toward 325 ° and 55 ° .

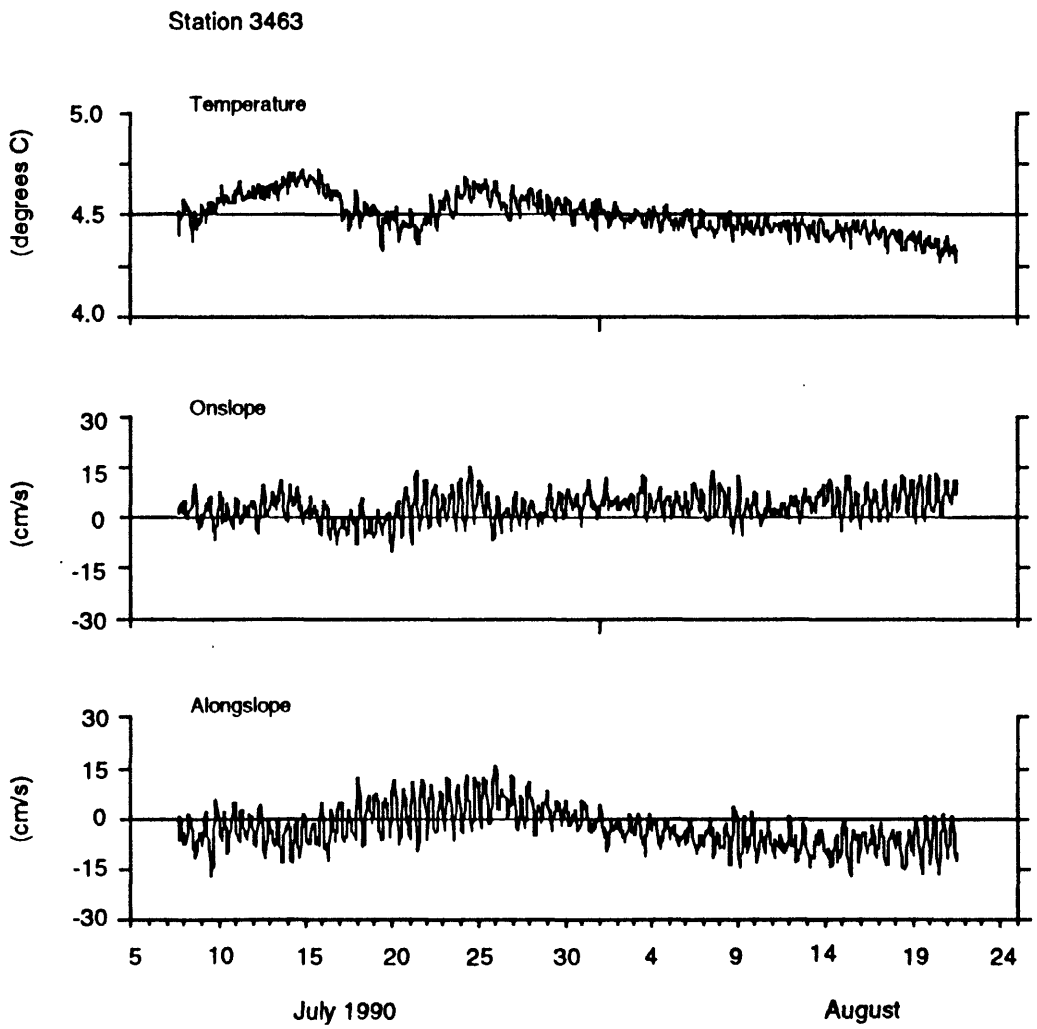

Figure B3. Hour-averaged current and temperature at the 885 m site. Positive along and onslope currents flow toward 325 ° and 55 ° .

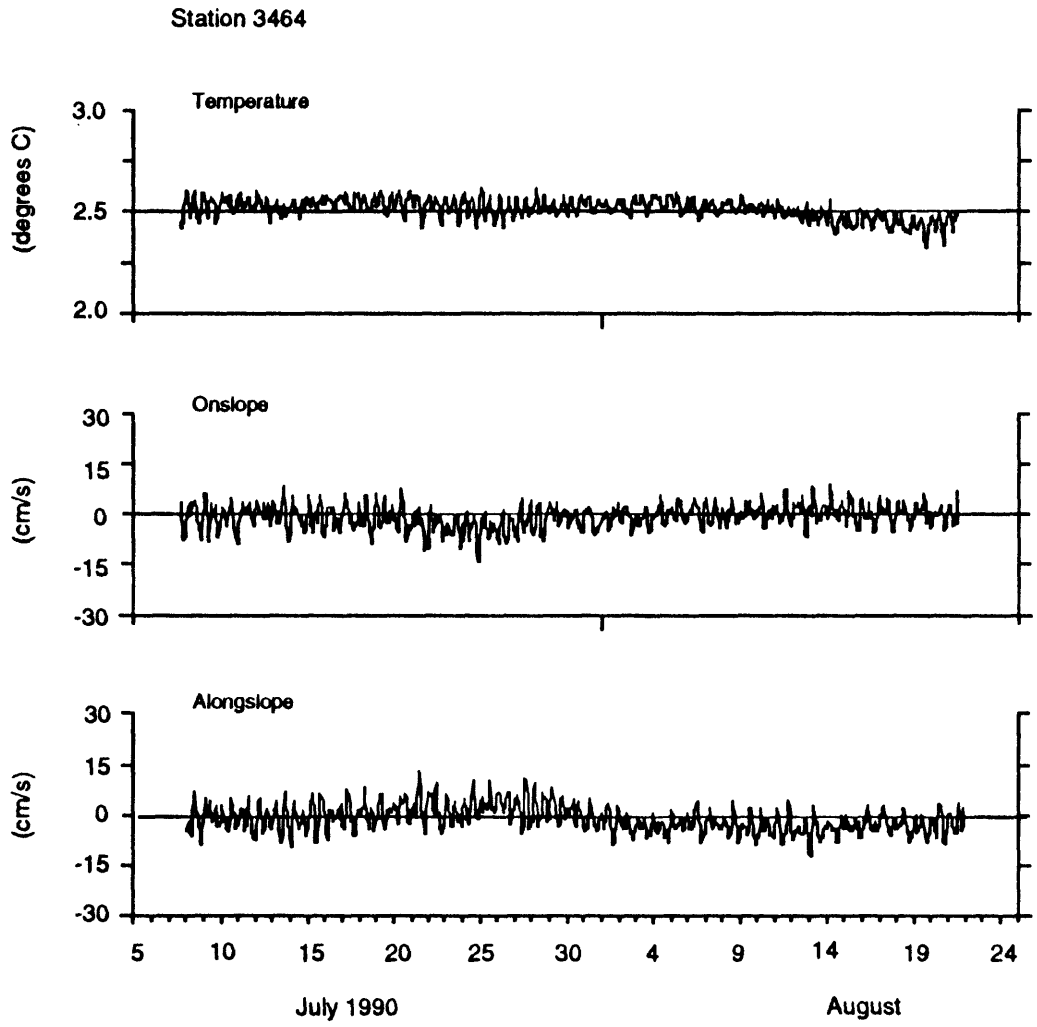

Figure B4. Hour-averaged current and temperature at the 1685 m site. Positive along and onslope currents flow toward 325 ° and 55 ° .

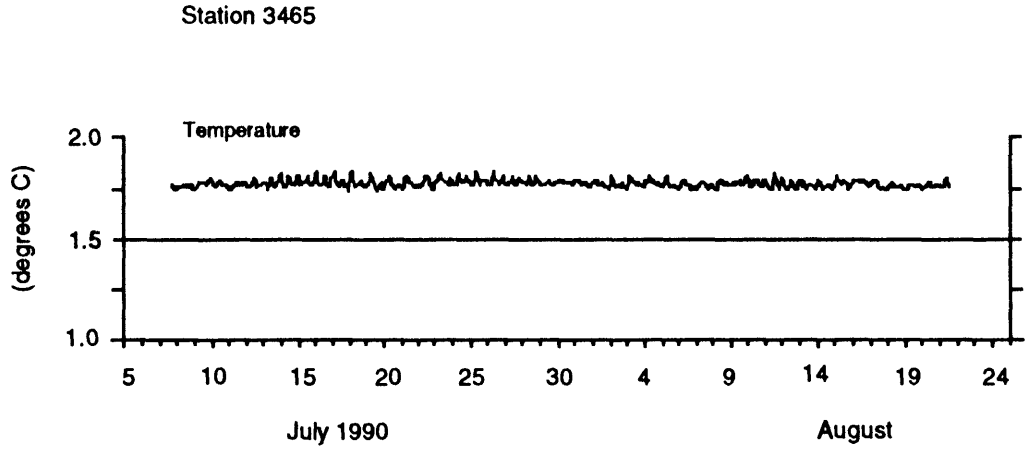

Figure B5. Hour-averaged temperature at the 2405 m site.

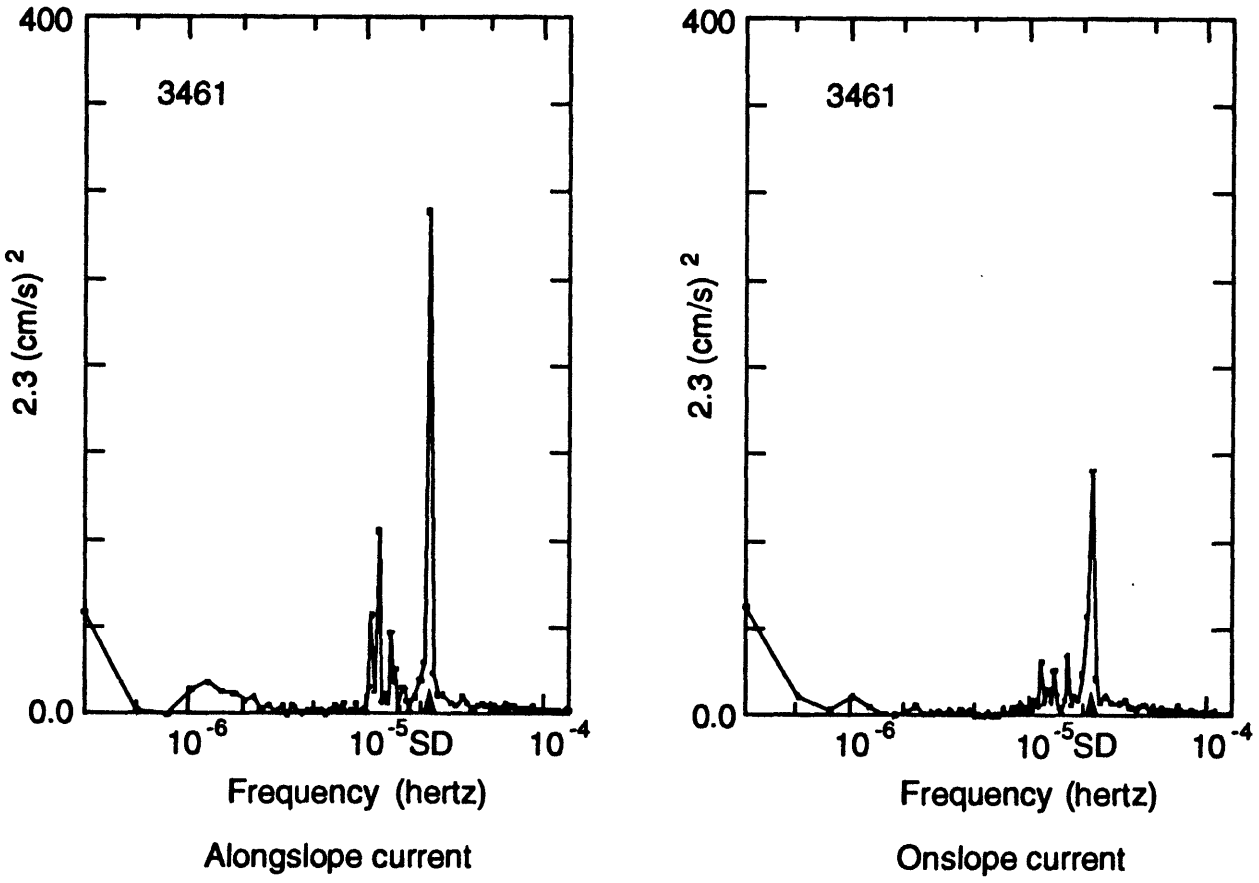

Figure C1. Variance-conserving periodogram of the along and onslope currents at the 285 m site SD denotes the semidiurnal tidal frequency.

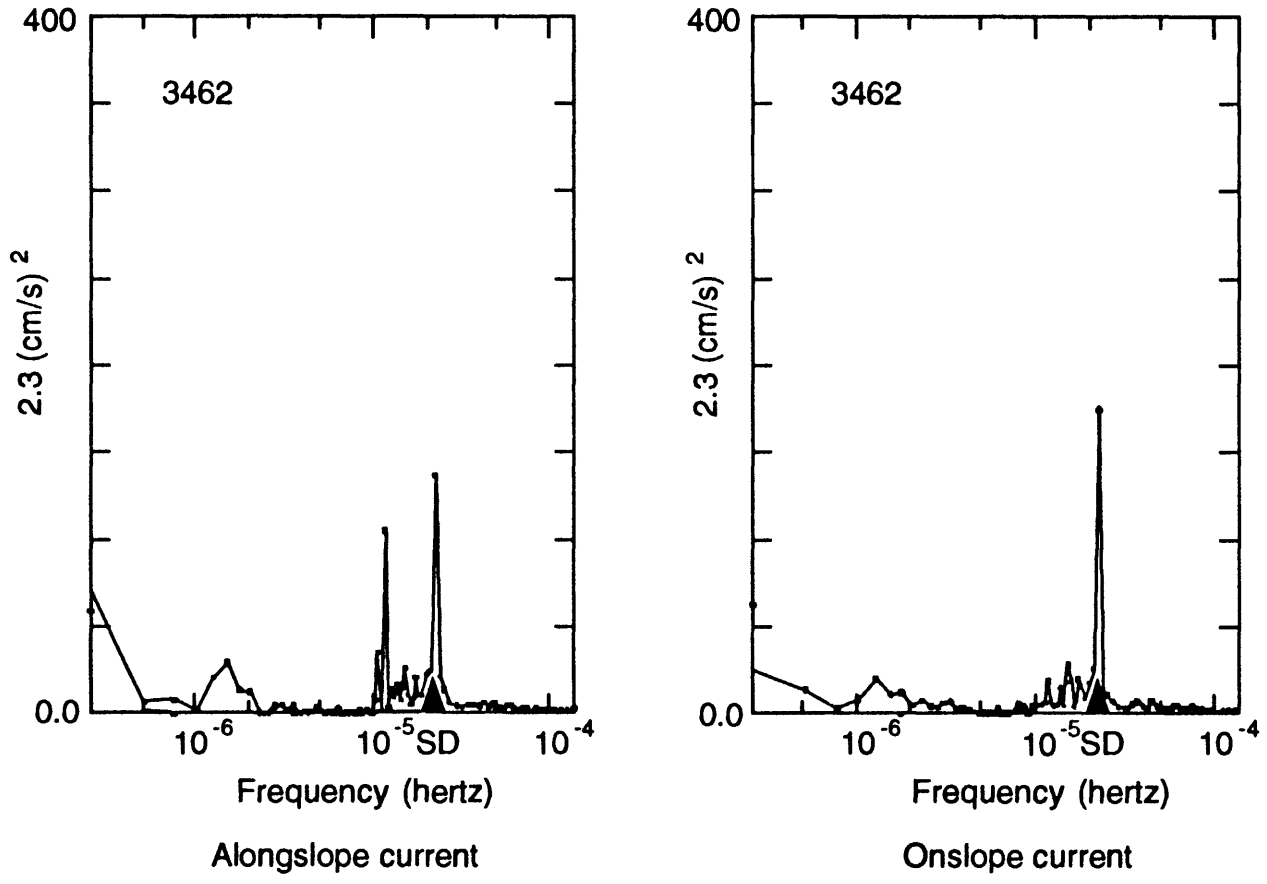

Figure C2. Variance-conserving periodogram of the along and onslope currents at the 485 m site. SD denotes the semidiurnal frequency

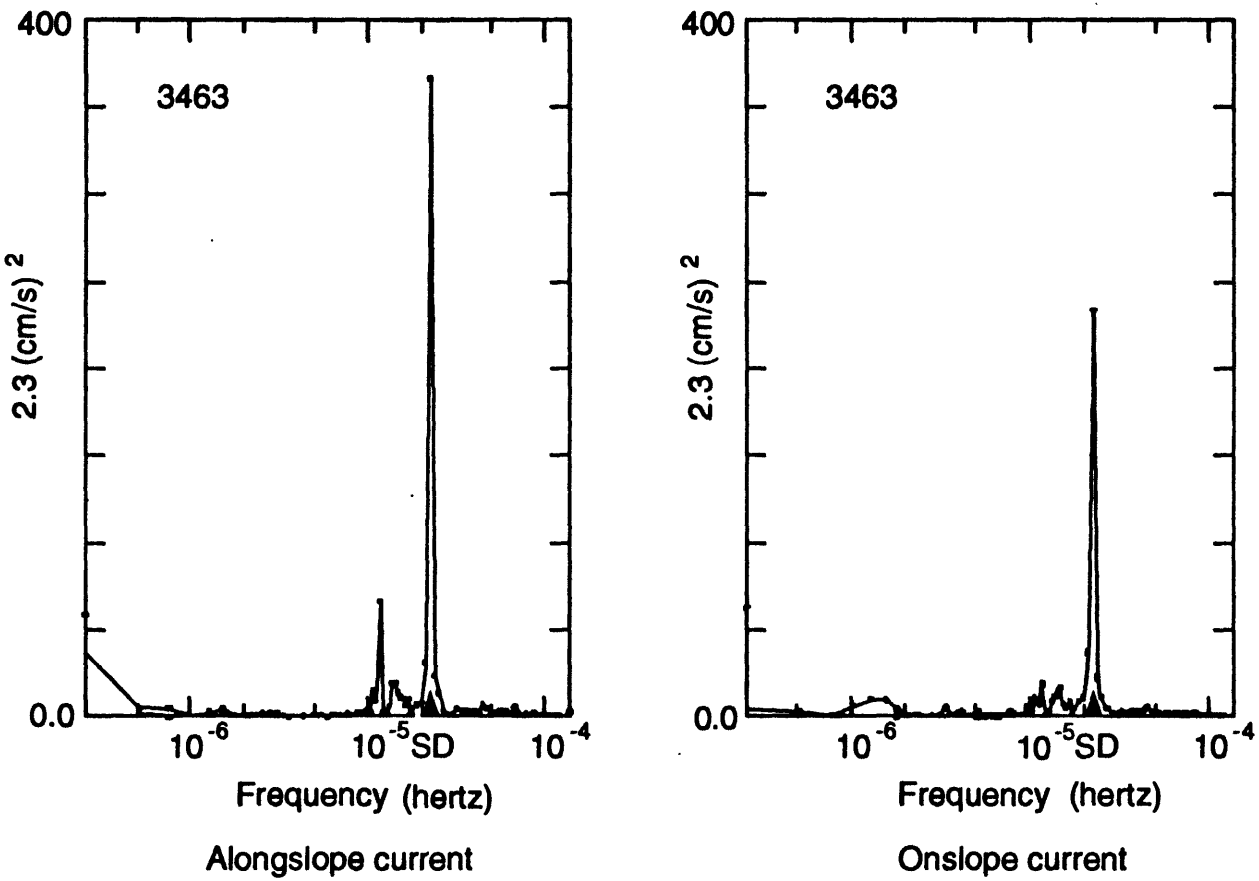

Figure C3. Variance-conserving periodogram of the along and onslope currents at the 885 m site. SD denotes the semidiurnal tidal frequency.

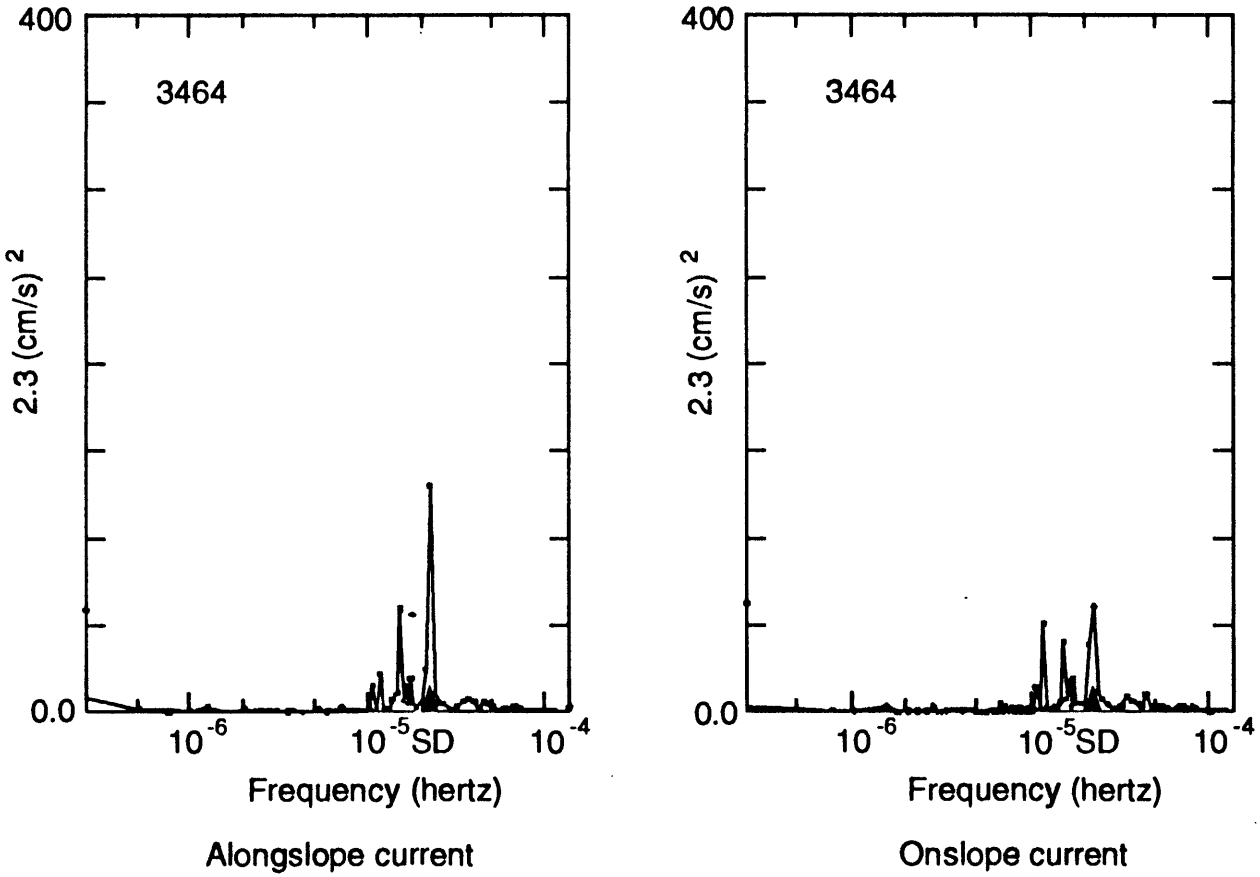

Figure C4. Variance-conserving periodogram of the along and onslope currents at the 1685 m site. SD denotes the semidiurnal tidal frequency.

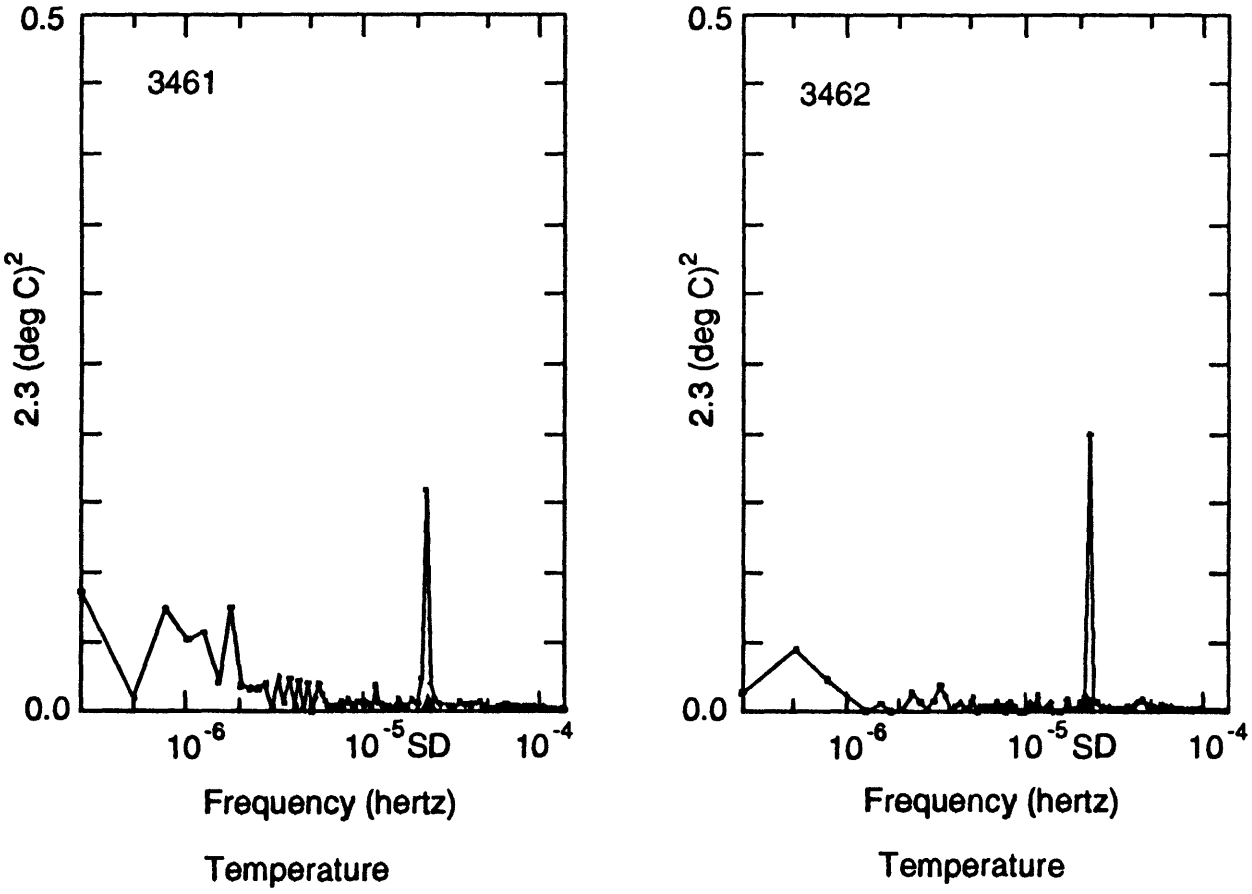

Figure C5. Variance-conserving periodogram of the temperature at the 285 and 485 m sites. SD denotes the semidiurnal frequency.

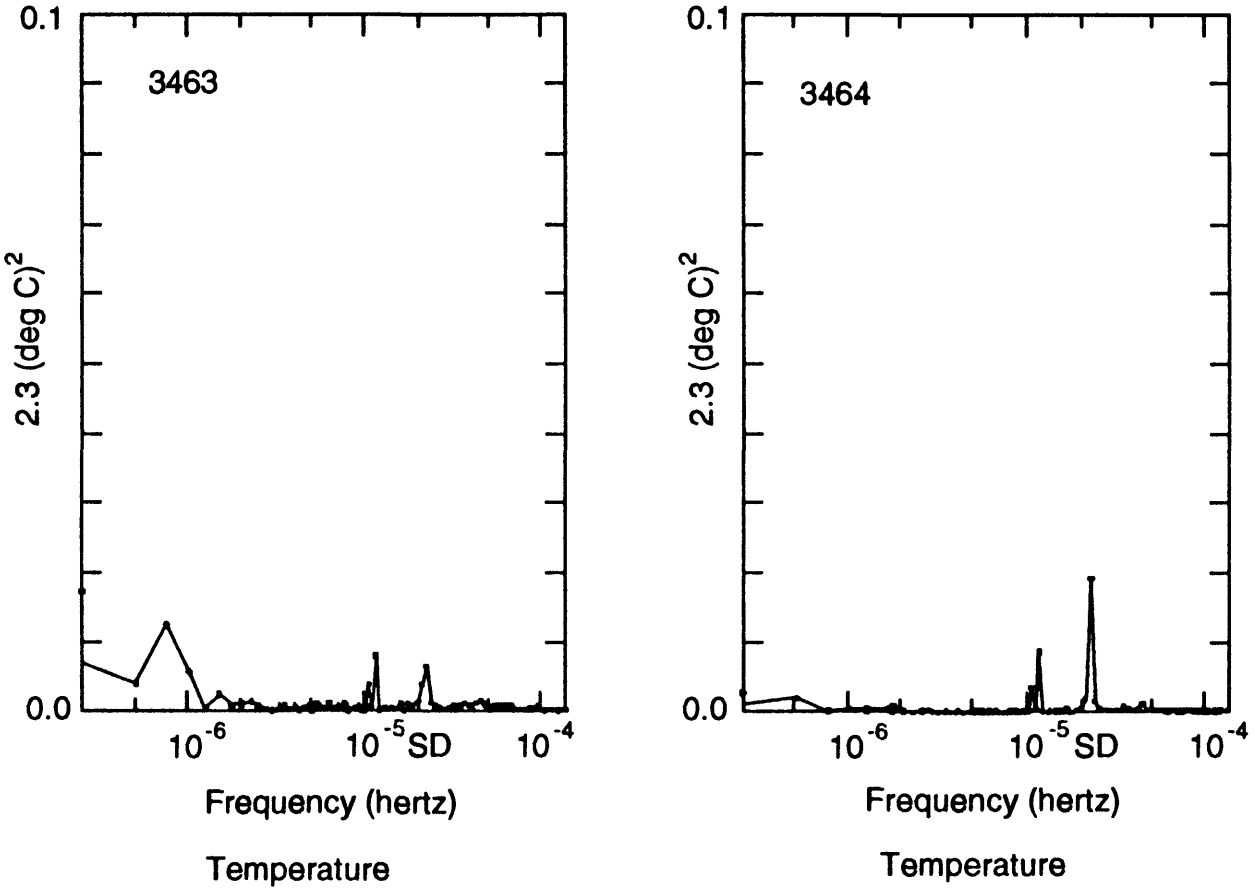

Figure C6. Variance-conserving periodogram of the temperature at the 885 and 1685 m sites. SD denotes the semidiurnal frequency.

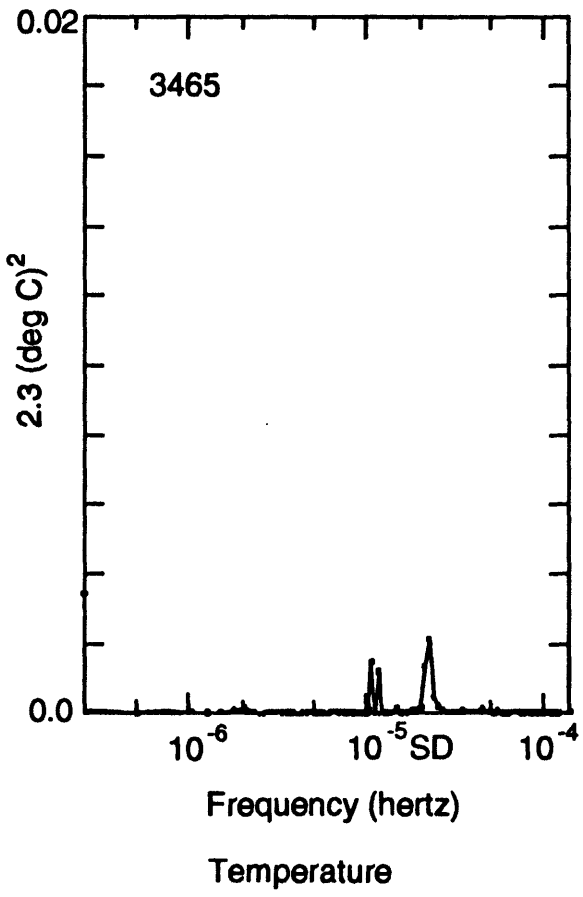

Figure C7. Variance-conserving periodogram of the temperature at the 2495 m sites. SD denotes the semidiurnal frequency.

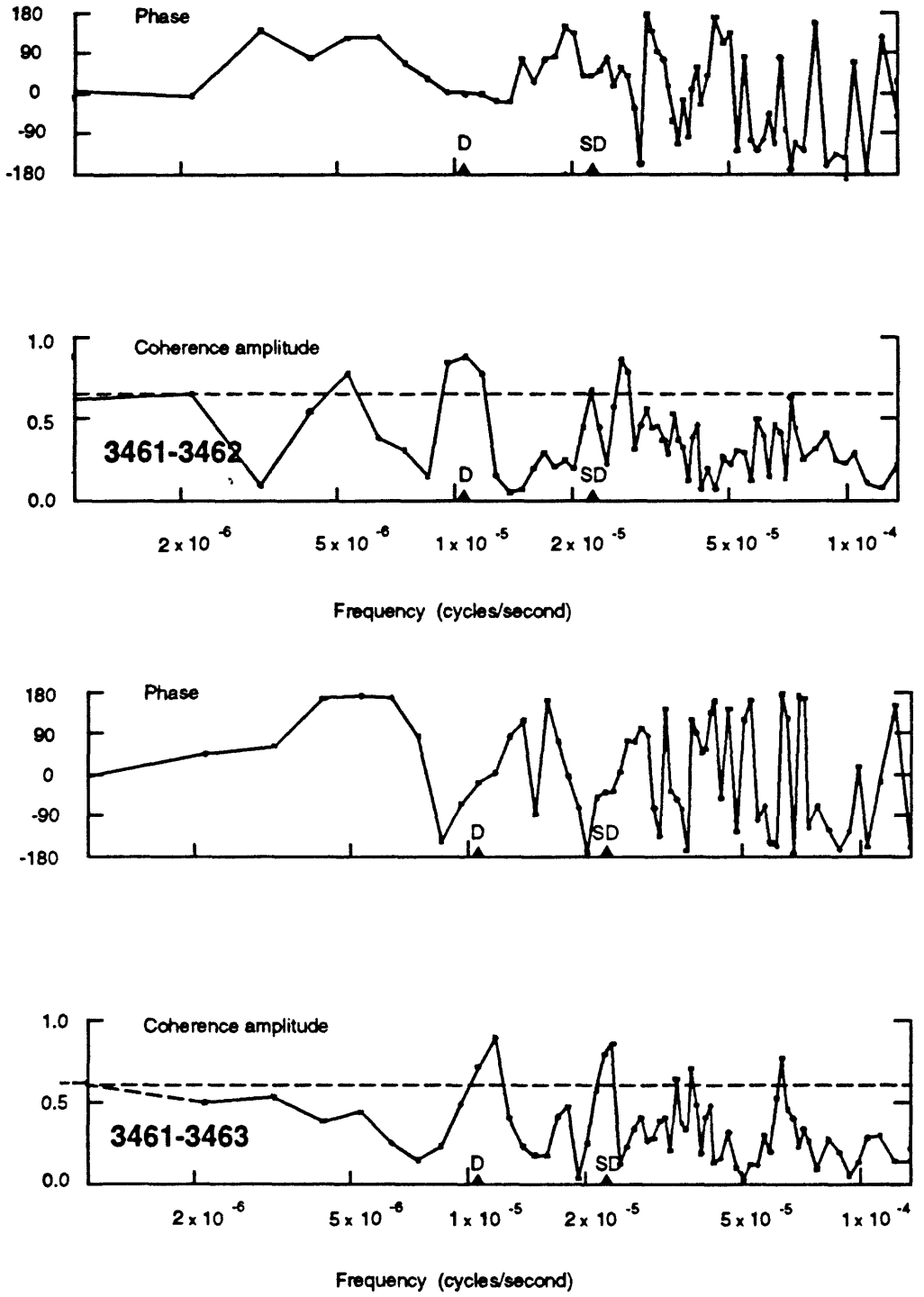

Figure C8. Coherence and phase between the alongslope currents. A negative phase indicates that the currents at the first site in an instrument pair lead the second. The coherence amplitude needs to be above the dashed line to be significant at the 95% confidence level.

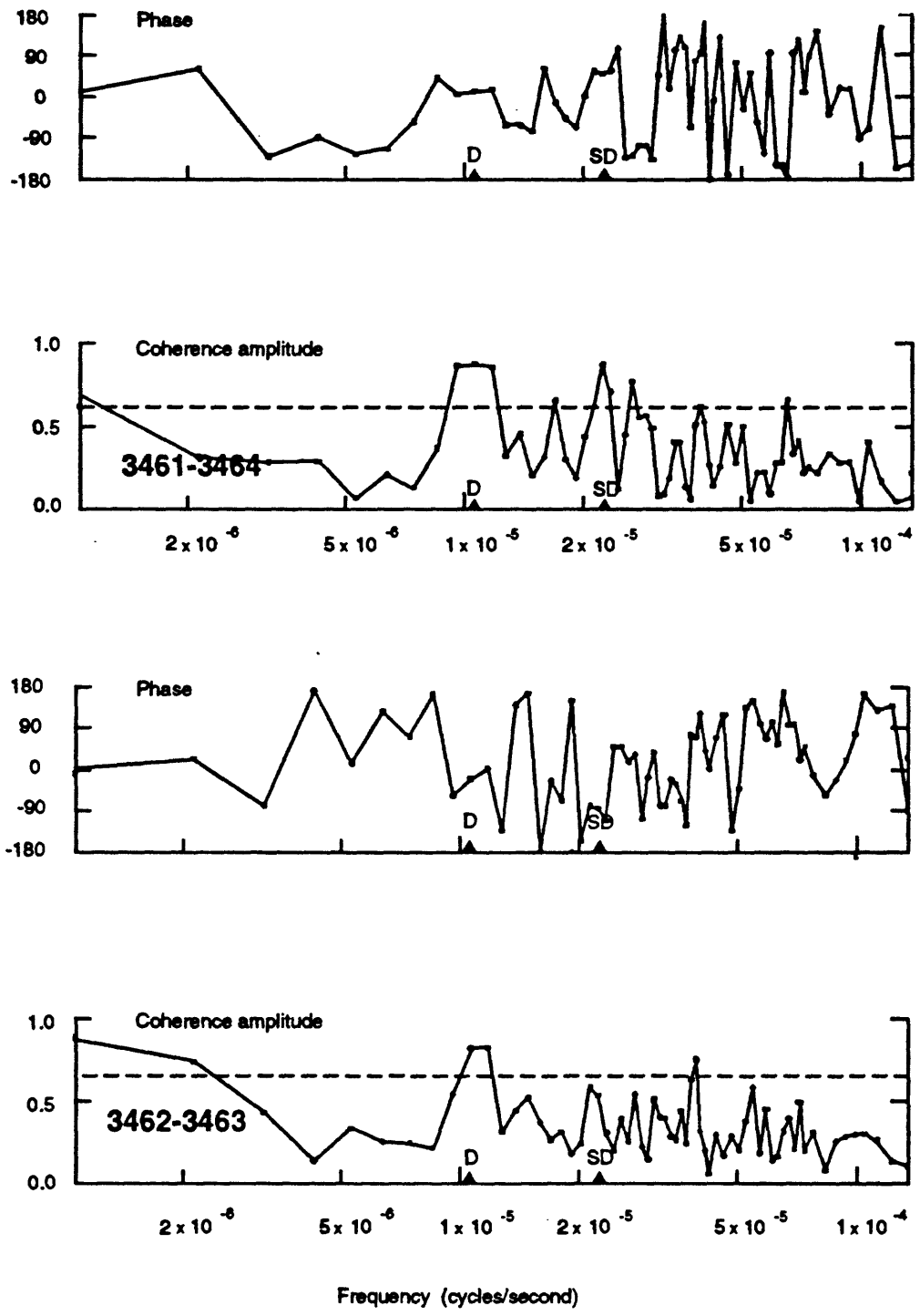

Figure C9. Coherence and phase between the alongslope currents. A negative phase indicates that the currents at the first site in an instrument pair lead the second. The coherence amplitude needs to be above the dashed line to be significant at the 95% confidence level.

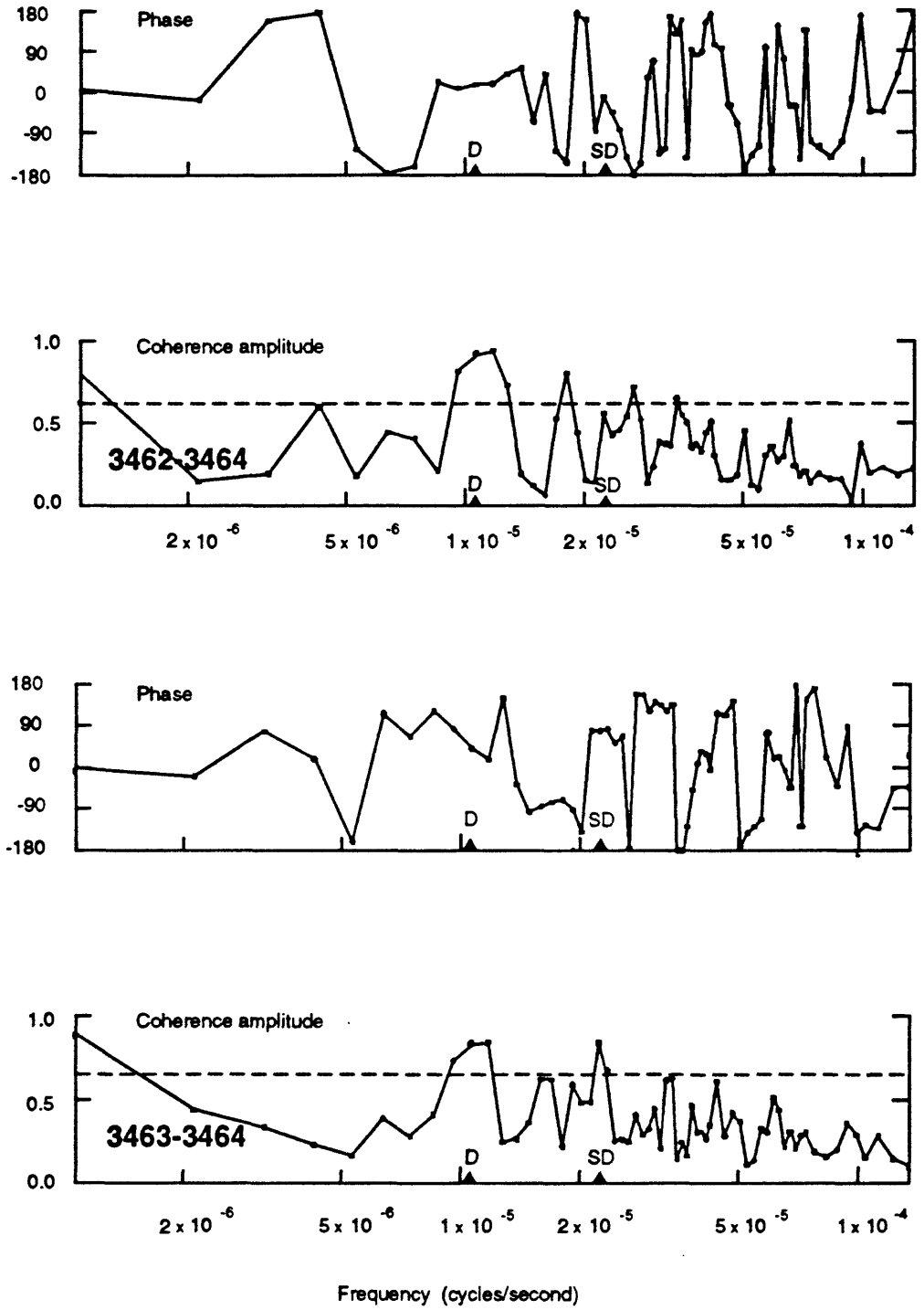

Figure C10. Coherence and phase between the alongslope currents. A negative phase indicates that the currents at the first site in an instrument pair lead the second. The coherence amplitude needs to be above the dashed line to be significant at the 95% confidence level.

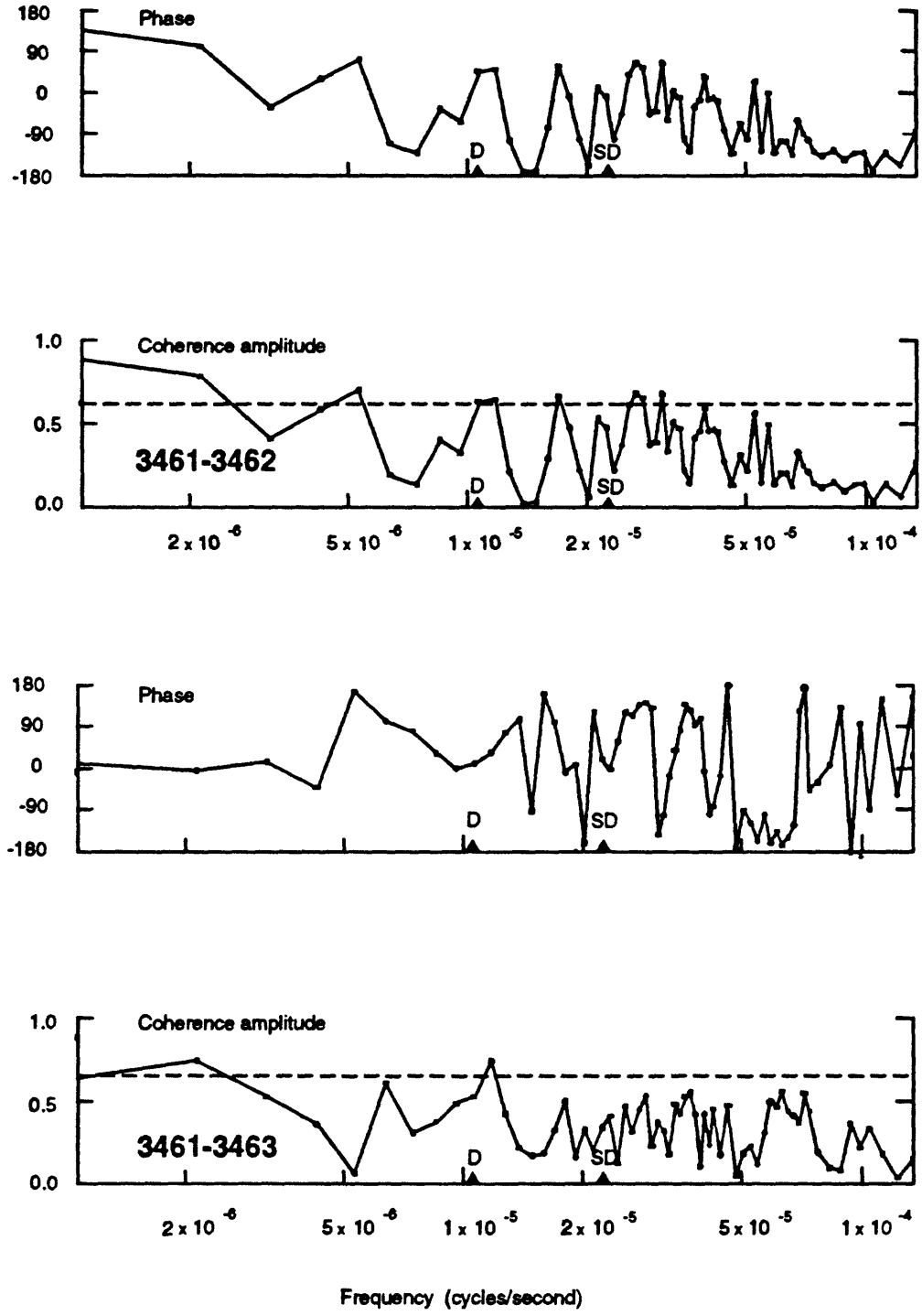

Figure C11. Coherence and phase between the onslope currents. A negative phase indicates that the currents at the first site in an instrument pair lead the second. The coherence amplitude needs to be above the dashed line to be significant at the 95% confidence level.

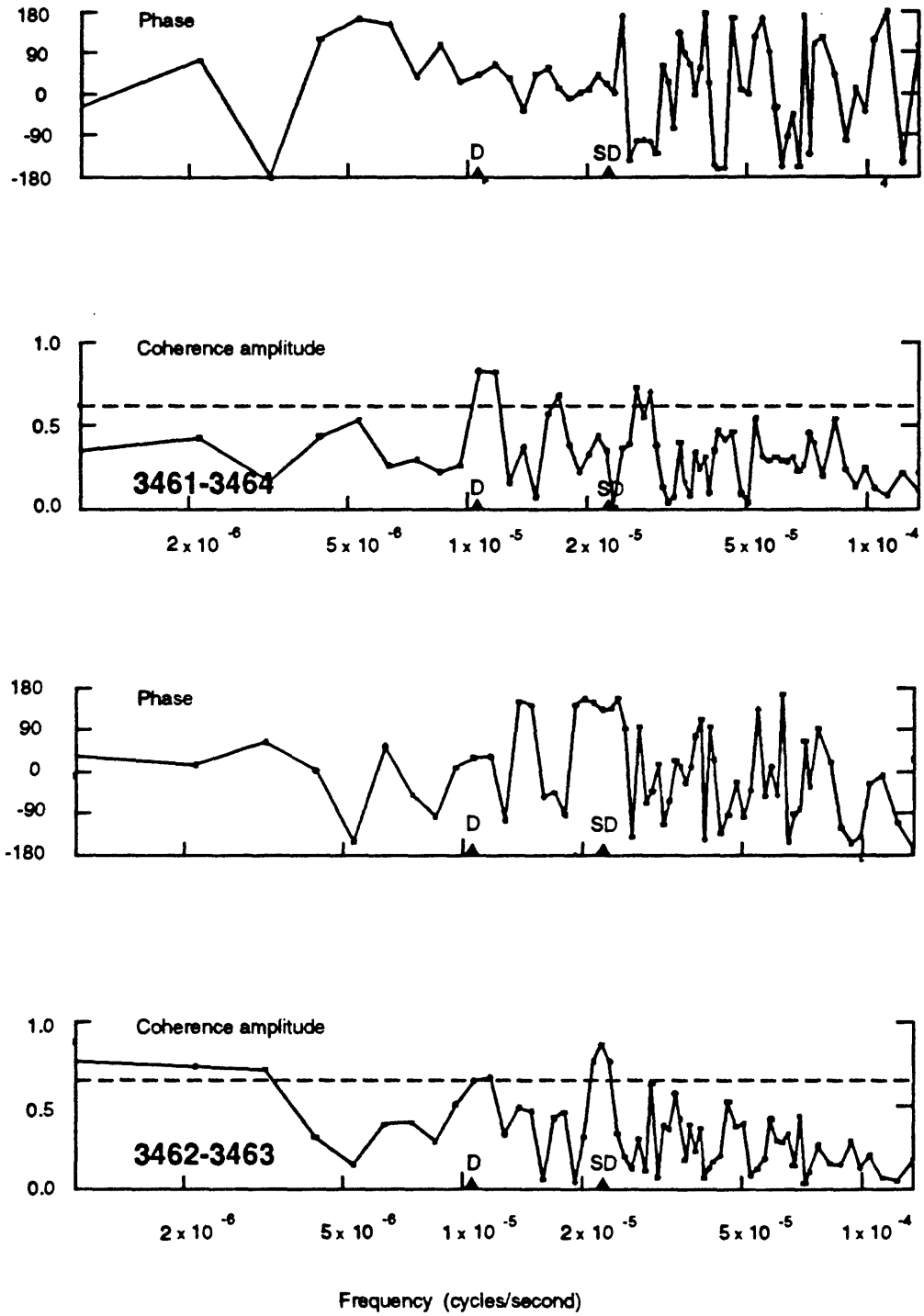

Figure C12. Coherence and phase between the onslope currents. A negative phase indicates that the currents at the first site in an instrument pair lead the second. The coherence amplitude needs to be above the dashed line to be significant at the 95% confidence level.

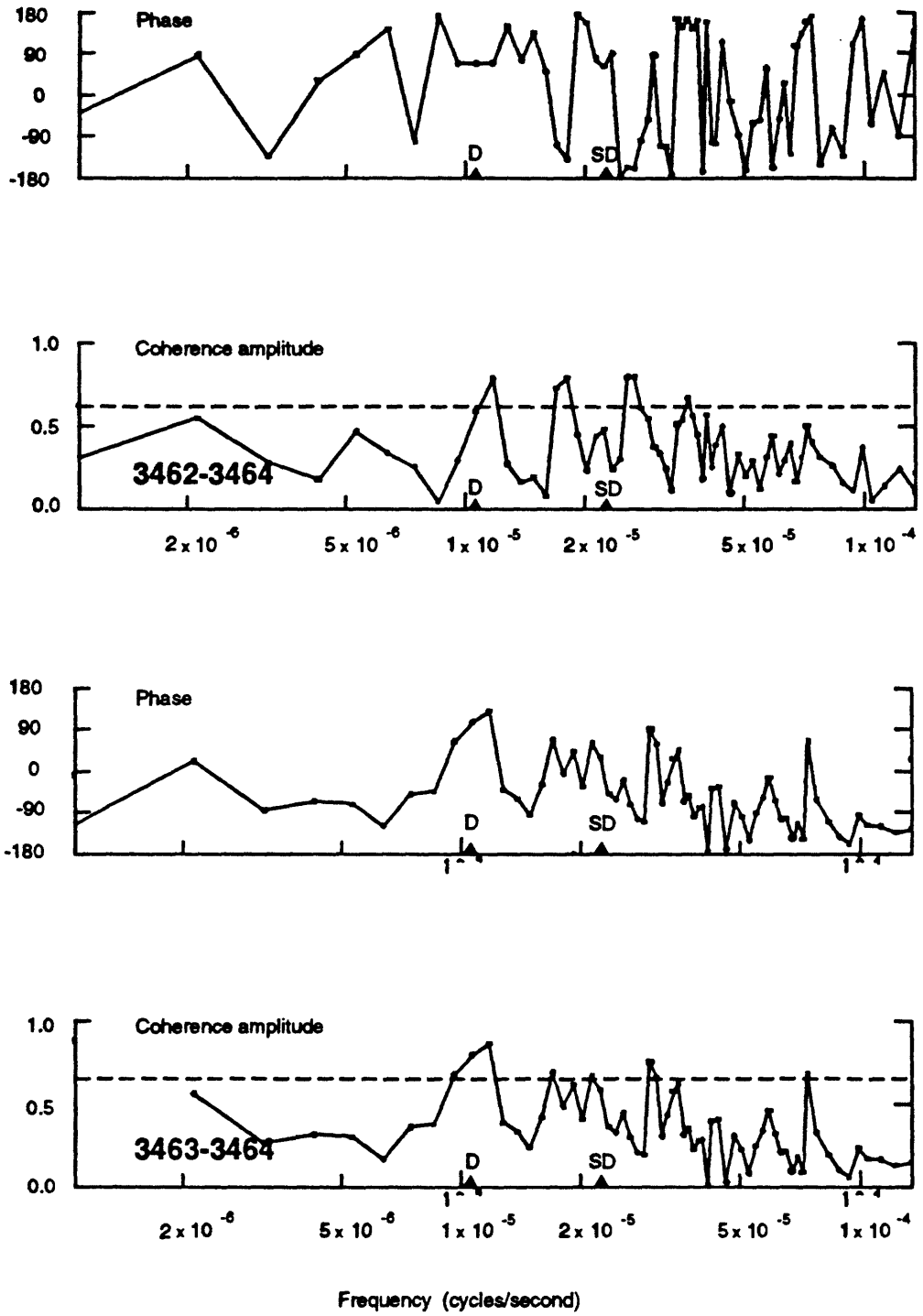

Figure C13. Coherence and phase between the onslope currents. A negative phase indicates that the currents at the first site in an instrument pair lead the second. The coherence amplitude needs to be above the dashed line to be significant at the 95% confidence level.